Landfast Ice Breakup Timing and Processes Along the Alaska Beaufort Sea Coast

Caroline Bell

A thesis

submitted in partial fulfillment of the

requirements for the degree of

Master of Science

University of Washington

2017

Committee:

Ignatius Rigor

James Morison

Susan Hautala

Jody Deming

Program Authorized to Offer Degree:

College of the Environment: School of Oceanography

University of Washington

Abstract

Landfast Ice Breakup Processes and Timing Along the Alaska Beaufort Sea Coast

Caroline Bell

Chair of the Supervisory Committee:
Dr. Ignatius Rigor
School of Oceanography

The record minimum in the extent of drifting sea ice on the Arctic Ocean was set in 2012, and the ten lowest retreats of summer sea ice were observed in the last decade. In this thesis we investigate whether there have been corresponding changes in the breakup of landfast sea ice using records from GPS buoys deployed on landfast sea ice in the Beaufort Sea region of Alaska between 2007 and 2015 to analyze the timing and cause of the breakup of landfast ice. Between two and five buoys were deployed each winter on stable landfast sea ice in two regions, Camden Bay and Harrison Bay, along the Alaskan Beaufort Coast. In addition to determining the start of landfast ice breakup, we used local surface winds, air temperature, water level, and air pressure data to examine the forces affecting breakup timing. Past studies have shown breakup is caused either by mechanical forcing from wind, currents or tides, or by thermal forcing due to above-freezing temperatures that cause ice to melt and drift away from the shore. We found the

average regional timing of breakup to start on June 6 for the 2007 through 2015 breakup seasons. This date follows the trend of an earlier breakup of landfast in this region, as it is five days earlier than observations from the 1990s to early 2000s and 24 days earlier than those from the 1970s. Although the earlier breakup trend is not statistically significant it does show continued changing conditions in the Beaufort Sea landfast ice regime. Exploring the processes affecting landfast ice breakup in our two sub-regions reveals landfast ice in Camden Bay beginning to break free on average on May 27 and in Harrison Bay on June 29. The large difference in breakup timing between the eastern and western Beaufort Sea coast can be attributed to different processes affecting the breakup. In Harrison Bay, break up was classified as thermally driven in all years. However, in Camden Bay break up was classified as mechanically forced in five out of the nine years of this study. These results differ from previous studies of the region, which report no link between atmospheric forcing processes and the timing of landfast ice breakup. This change is most likely related to the overall transition of Arctic sea ice to a younger, thinner ice pack, which now provides a weaker buttress for the landfast sea ice.

TABLE OF CONTENTS

LIST OF FIGURES

LIST OF TABLES

ACKNOWLEDGEMENTS

I would first like to thank the many professors and colleagues who helped me through this Master's process namely: Ignatius Rigor, James Morison, Susan Hautala, Jody Deming, Rosalind Echols, and Hillary Scannell.

I am incredibly grateful for the opportunity to see first-hand sea ice and landfast ice in the Arctic Ocean; thank you, Ignatius Rigor, for ensuring I was able to experience Arctic field work.

Thank you to my parents, Janiece and Peter for their encouragement and support, and instilling in me the importance of education.

I am grateful for the constant love and attention of my pug, Aiden, who will be happy to cuddle on my lap again without having to push a laptop or notebook out of the way first.

Finally, I cannot express how thankful I am for the love and support of my husband, Dan. Thank you for understanding and supporting my decision to attend UW, thank you for keeping me grounded and having confidence in me when I did not. He has always believed in me and encouraged me to accomplish things I did not think I was capable of achieving.

Chapter 1. INTRODUCTION

The areal extent of Arctic sea ice has been declining since satellite records have been kept, beginning in the early 1980s, and is well quantified through a variety of satellite measurement methods. From satellite data analyzed between 1979 and 2013, the overall Arctic sea ice cover has declined by 14% per decade (Stroeve et al., 2014). Minimum sea ice extent, or surface area covered, occurs at the end of summer melt in September each year over the past three decades there has been increased open water and less sea ice coverage (Figure 1-1). In addition to the declining total area of sea ice, other properties and characteristic of the sea ice are changing; there is thinner ice, declining multi-year ice, and a longer open water season (Johnson & Eiken, 2016). Fewer studies have analyzed and cataloged the landfast ice which is the non-permanent sea ice that forms near shore each winter and remains through late spring or early summer. Landfast ice is important to limiting coastline erosion during winter storms (Reimnitz et al., 1994; Reimnitz, 2002), providing a stable area for Inuit subsistence hunting and fishing (Meier et al., 2014; Eicken et al., 2014), and a platform for offshore oil and gas drilling (Barry et al., 1979; Vaudry, 1989; Vaudry, 2006; Mahoney et al. 2006; Mahoney et al., 2007; Petrich et al., 2012). Multiple studies of breakup timing and landfast ice movement were first conducted in the 1970s –1980s along the Alaska Beaufort Sea coast using both satellite images of landfast ice and buoys deployed on the ice to track movement (Barry et al., 1979; Vaudry, 1989; Vaudry, 2006). More recent studies in the late 1990s through early 2000s of landfast ice movement utilizing satellite images report breakup beginning up to two weeks earlier than in the 1970s and 1980s (Mahoney et al., 2007, 2014; Johnson & Eicken 2016). Additionally, a study of landfast ice in the Chukchi Sea off Barrow, AK, that utilized a combination of local radar, camera images, and satellite

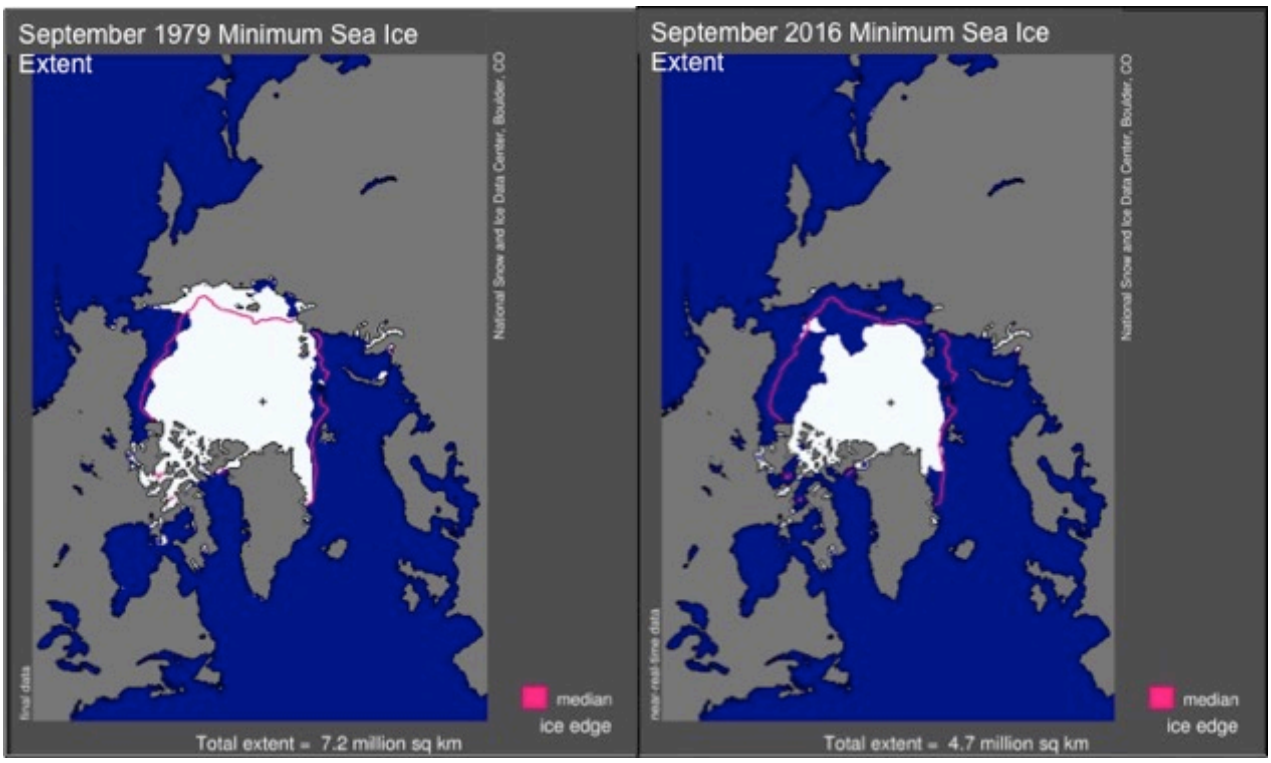

Figure 1-1 Minimum sea ice extent from NSIDC (nsidc.org/data/docs/noaa/g02135_seaice_index/#monthly_extent_image) for September 1979 (left) and September 2016 (right). The pink line shows the median minimum sea ice extent 1980–2010.

images, along with weather and current observations between 2000 and 2010, defined breakup as either mechanical (ice breakup forced by winds, currents, or tides) or thermal (ice melting in place) (Petrich et al., 2012). Typically, when thermal processes have caused landfast ice breakup, the ice stays anchored by offshore ridges until melting in place (Mahoney et al., 2007; Petrich et al., 2012). Petrich et al., (2012) also report that mechanical processes caused breakup in four of the years studied, and thermal processes in six. This thesis 1) examines the timing of landfast ice breakup over the past decade using Surface Velocity Profiler (SVP) buoys placed on the ice and 2) determines the cause of breakup as either thermal or mechanical. The analysis of velocity derived from hourly latitude and longitude data from sea ice buoys provided the breakup timing of the sea ice. Additionally, sea surface heights from a NOAA tide gauge at Prudhoe

Bay, AK, and North Atlantic Regional Reanalysis (NARR) surface air temperature and wind speeds from the National Center for Environmental Predictions (NCEP) provide data for the forcing analysis. The regional focus of this analysis is along the Beaufort Sea coast of Alaska.

1.1 CHANGING CONDITIONS IN ARCTIC SEA ICE

Two key indicators of total Arctic sea ice are the annual minimum and maximum extent and the thickness or age of the ice. The minimum and maximum sea ice extents, the minimum and maximum surface area covered by sea ice, typically occur in September and March, respectively. Sea ice minimum and maximum extents have been measured by satellites since 1979. Data analysis available from the National Snow and Ice Data Center shows that the minimum summer ice extent has been shrinking over the past several decades (Figure 1-1). Record minimum ice extents were first observed in 2007 and again in 2012, which is the current record minimum extent (Figure 1-2). The recent trends over the past decades show sea ice extent on the decline. Although a record summer sea ice extent minimum did not occur in 2016, it was among the lowest 10 minimum extents. The Beaufort Sea is one of the regions of the Arctic where summer sea ice extent has decreased the greatest (National Research Council, 2012).

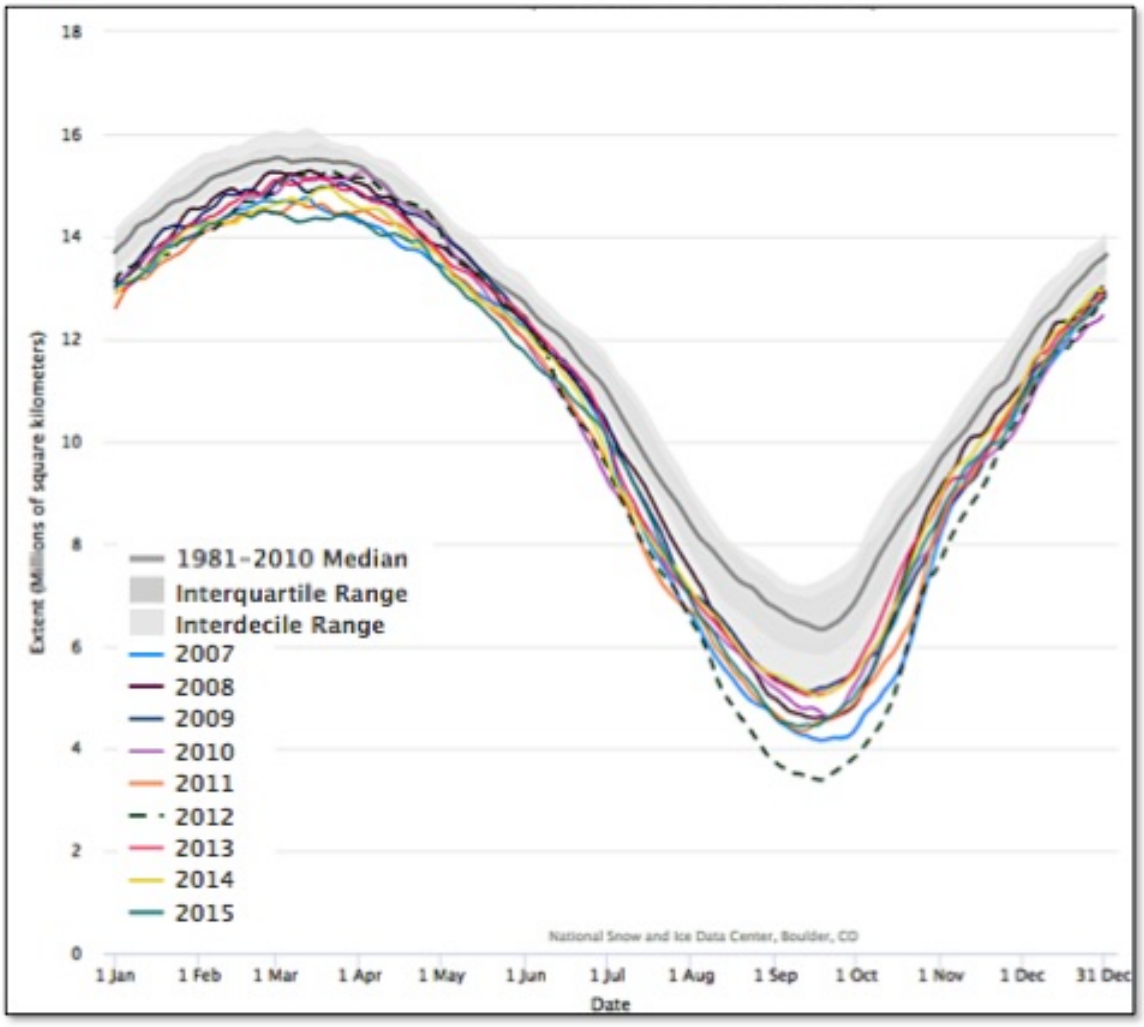

Figure 1-2 Annual Arctic Sea Ice extent 2007–2015 compared with 1981–2010 median extent from NSIDC (http://nsidc.org/arcticseaicenews/charctic-interactive-sea-ice-graph/).

In addition to shrinking ice cover the duration of the melt and open water seasons are increasing. Along the Beaufort Sea the melt season ranges in length from 3–5 months with large interannual variability (Stroeve et al., 2014). Between 1979 and 2013 Stroeve et al. (2014) found continuous melt in the Beaufort Sea to occur 2.7 days per decade earlier, and in the central Arctic 1.7 days earlier per decade. The onset of freezing was also found to begin later over the 1979–2013 period, leading to a 9 day per decade longer open water period (Stroeve et al., 2014). A shorter ice-covered period in the Arctic leads to increased warming of the open ocean from

absorption of incoming solar radiation. The heating of surface waters causes a higher amount of energy to be removed by cooling before sea ice can form again in the fall.

In conjunction with changing conditions to sea ice in the Arctic are changing atmospheric conditions over the Arctic Ocean and coastal seas. A semi-permanent high-pressure region known as the Beaufort High, controls surface winds along the Alaskan coast. Winds are predominantly out of the east and roughly parallel the Beaufort Sea coast (Williams & Carmack, 2015) because of the anticyclonic rotation around the high-pressure zone. Recent studies no longer demonstrate a clear link between the Arctic Oscillation, an index of the variability of the Beaufort High, and sea ice loss (Petty et al., 2016). Between 1980 and 2013 Petty et al. (2016) report a strong correlation between the Beaufort Sea ice drift and wind stress curl. They found the strongest intensification in the Beaufort Sea ice drift between 2007 and 2010 with weakening wind and ice drift observed since 2010.

1.2 Landfast Sea Ice Description

Around the coastal zones and marginal seas of the Arctic Ocean sea ice grows outward from shore as air and water temperatures drop below the freezing point for seawater, around –1.8 ℃. This sea ice, called landfast or shorefast ice, is seasonal and typically present eight to nine months per year. In the literature, landfast ice or fast ice is defined by a number of slightly different criteria. For example, Barry et al. (1979) define it as 1) sea ice that is relatively stable near shore for a specific time period, 2) a continuous ice sheet from coast seaward, and 3) the continuous sheet that is grounded or bound at its seaward edge by a near continuous zone of grounded ice. Mahoney et al. (2005) define it as 1) sea ice that is contiguous with the coast, and 2) sea ice that lacks detectable motion for approximately 20 days. Petrich et al. (2012) further

defined landfast ice as an aggregate of grounded pressure ridges and attached shoreward level and rubble ice. The common thread is that landfast ice is attached to the shore extending seaward and held by grounded sea ice. Additionally, this ice is stable for a period of time, which some have defined in terms of the timeframes of satellite images (Barry et al., 1979; Mahoney et al., 2014).

Throughout the coastal Arctic Ocean the length of ice-free coastal regimes to ice formation varies slightly, and in some regions of the Canadian Archipelago landfast ice remains year round (Melling, 2002; Mahoney et al., 2007; Howell et al., 2009; Yu et al., 2013). Along the Beaufort Sea coast, landfast ice begins to form when the air temperature remains consistently below –1.0 ℃, typically in mid- to late October (Mahoney et al., 2014; Barry et al., 1979). As seawater in shallow, nearshore areas drops in temperature its freezing point, ice begins to form and grow outward from the coastline. This landfast ice continues to grow throughout the late fall and early spring. Additionally, in the Beaufort Sea region, mobile pack ice grounds as it is either blown by surface winds or pushed by currents into shallow shelf waters. This grounded ice forms a seaward edge of the landfast ice and helps to stabilize the ice shoreward of it (Barry et al., 1979; Reimnitz et al., 1994; Mahoney et al., 2006, 2007, 2014; Petrich et al., 2012).

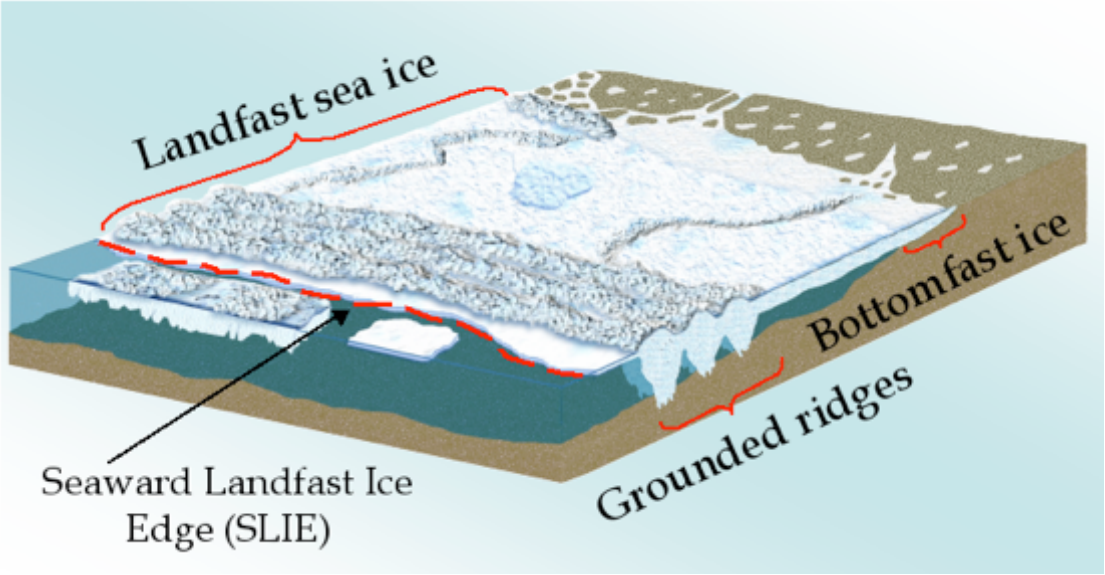

Figure 1-3 Representation of landfast ice (boemre-new.gina.alaska.edu/). Highlighted are the bottomfast ice area where ice freezes the full depth of the sea, grounded ridges toward the seaward edge, the seaward landfast ice edge (SLIE), which here extends slightly farther than the grounded ridges. The entire region from SLIE to shore is considered landfast ice.

There are a variety of zones in the landfast ice region that are defined based on how the ice is attached to the shore or bottom (Figure 1-3). Typically, the zone between 0.0 and 2.0 m depth is considered the bottomfast ice zone where sea ice freezes the whole depth from the surface to seabed (Reimnitz et al., 1978; Mahoney et al., 2006). Next is a region of surface landfast ice, not frozen to the seabed, that is stable because of the connection to the bottomfast ice near shore (Mahoney et al., 2006; Reimnitz et al., 1979; Reimnitz 2000). Due to tidal fluctuations and the connection between bottomfast ice and surface landfast ice in the northern Alaska region, it is common to see tidal cracks in the ice close to shore (Mahoney et al., 2006). At the shoreward edge of the landfast ice, there is a zone of grounded ridges typically found between the 10-m and 30-m isobaths (Reimnitz et al., 1978, Mahoney et al., 2007). The ridges are created by either the pack ice drifting into shallow water or sea ice deforming in place enough to ground the keel of the ice (Reimnitz et al., 1994; Mahoney et al., 2006). These

grounded ridges with their keels held fast to the sea floor create the strong link between the farthest extent of landfast ice and the 20-m isobath (Mahoney et al., 2007). Conditions in the Beaufort Sea, including anticyclonic circulation of winds and pack ice, can force thickening of ice up to 40 m thick at the seaward edge of landfast ice (Reimnitz et al., 1994). From year to year the farthest seaward distance of landfast ice from shore is called the seaward landfast ice edge (SLIE) (Figure 1-3). Another key feature of the landfast ice zone in the Beaufort Sea region is a shear zone between the grounded pressure ridges and the mobile pack ice (Reimnitz et al., 1978). This region is a highly deformed region of ice (Reimnitz et al., 1978, 1994), which can either extend the SLIE or cause breakout events depending on the season and the forcing of the pack ice drift.

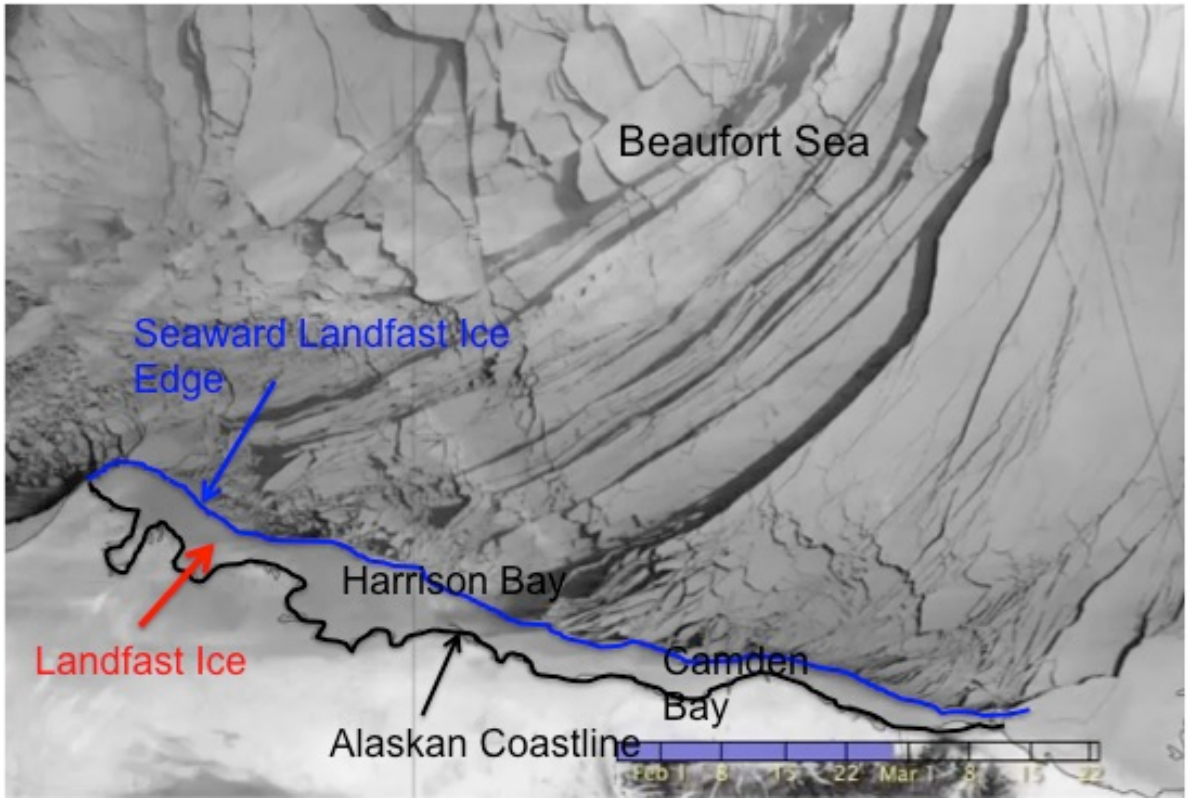

Figure 1-4 Visible infrared image of landfast ice along the Alaska Beaufort Sea coast, outlined in black (earthobservatory.nasa.go). Seaward landfast ice extent outlined in blue. Pack ice is seen as cracking sheets of ice in the Beaufort Sea. Image is from late February 2013.

Landfast ice remains relatively stable until late spring or early summer. When surface air temperatures begin to rise above freezing landfast ice begins to decay in place. This ice can remain fast to the shore until it melts completely, which is classified as thermal breakup, or strong storms or surge events can unground the decaying ridges in what is termed mechanical breakup (Mahoney et al., 2007, 2014; Petrich et al., 2012; Jones et al., 2016). Incoming solar radiation acts to weaken and melt the landfast ice and can begin to warm the seawater underneath it. If there are no strong mechanical events to break free the grounded pressure ridge, thermal heating processes will melt them enough to float freely. Additionally, in river delta regions spring thaw can impact the landfast ice by flooding shallow regions where bottomfast ice is attached (Reimnitz, 2002). Over the past decade throughout the whole Arctic region, there has been a trend towards earlier landfast ice breakup (Yu et al., 2013; Mahoney et al., 2014; Selyuzhenok et al., 2015; Johnson & Eicken, 2016).

1.3 Characteristics of the Alaska Beaufort Sea Coast

The Beaufort Sea coast of Alaska extends from the Alaska–Canada border in the east to Point Barrow, AK in the west. Prominent features include bays, barrier islands, river deltas, and headlands. This area has a narrow shelf extending on average 65 km from shore, but in some locations is only 15 km wide, with a shelfbreak depth of 65 m (Williams & Carmack, 2015). The Beaufort Gyre circulation dominates the region and forces the general current and sea ice drift in an anticyclonic pattern (Petty et al., 2016). Winds along the Beaufort Sea coast are typically easterly parallel to the coast, driving the westward flow of the southern part of the Beaufort Gyre. Strong seasonal storms can shift the wind temporarily, but throughout the year the winds are predominantly out of the east. Additionally, near shore, there are coastal currents that vary seasonally with stronger currents during the summer open water season, and minimal

currents during the ice-covered season. During the winter ice-covered season coastal currents are weak and tidally driven (Weingartner et al., 2005), on average reaching only 3 cm s^{-1} (Williams & Carmack, 2015). Results from a drifter study in the late 1970s showed weak under ice currents, which predominantly flowed shoreward while ice cover persisted (Matthews, 1981). Tides along the Beaufort Sea shelf are considered mixed but mainly semidiurnal with low tide range, < 0.1 m amplitude (Huang et al., 2011). Semidiurnal tides are those that have two high and two low waters a day, where the amplitude of the highs and lows are roughly equal.

The anticyclonic Beaufort Gyre rotation forces pack ice in the Beaufort Sea to interact with landfast ice along the Alaska coast. As the pack ice grows during late fall and early winter, some of it can get pushed into the shallow shelf waters of the Alaska coast (Reimnitz et al., 1978; Barry et al., 1979). The main ice drift direction is along shore throughout the winter and spring. The constant motion of pack ice forced by winds and currents in the Beaufort Gyre cause the ice to pile up into rubble fields. Also, pressure ridges can form extending upwards with keels below the water level, making the ice quite thick in some places. Additionally, as sea ice moves into shallow water where ice keels ground on the seabed, further deformation can occur.

Mahoney et al. (2014) examined the effects of headlands and embayments of the Beaufort Sea coastline on the growth and decay of landfast ice, and report that year-to-year the SLIE had a more consistent location near headlands, shoals, and areas where isobaths extended further from shore. In these common areas the mean SLIE aligned closely with the 20-m isobaths, which shows the link between the farthest edge of the landfast and seafloor bathymetry (Mahoney et al., 2007, 2014). Each of these characteristics affects the formation, maintenance,

and breakup of landfast ice in the region. However, there are also key differences between the eastern and western Beaufort Sea regions. In the eastern region, the ice-free season is typically longer, partly due to an influx of fresh water from the Mackenzie River delta system and partly due to the narrower landfast ice region (Vaudry, 2006). The 20-m isobath is closer to the shoreline in the eastern Beaufort Sea, extending 5–9 km from shore in areas to the east of Camden Bay, and extending 18–30 km wide in Camden Bay (Vaudry, 2006). In the western Beaufort Sea region the 20-m isobath extens up to 40 km from shore and typically fall between 30 and 38 km (Vaudry, 2006).

The location of the 20-m isobath is important to landfast ice for many reasons. The 20-m isobath is a good reference point for the farthest extent that landfast ice grows from the coast in a season. The sea ice with deep keels from pressure ridging and rubbling can ground and stabilize the landfast ice. Also, in areas where there are shoals offshore at or above the 20-m isobaths, which are prominent in the western region, the seaward landfast ice edge can extend farther from shore when multi-year ice floes ground on these shallow areas (Vaudry, 2006; Mahoney et al., 2007, 2014). Observations of grounded sea ice and landfast ice in the Beaufort Sea region have shown it typically extends to water depths of 18–30m. As discussed by Reimnitz (1978), stable extensions can form beyond the edge of the grounded landfast zone. It is important to note that these areas beyond the grounded keels are more susceptible to early breakout events and intrusions by pack ice.

Breakup of landfast ice along the northern Alaska coast has trended earlier since the late 1970s: during 1973 to 1977 breakup began on average on June 30 (Barry et al., 1979); during

1996–2003 breakup began on average on June 11 (Mahoney et al., 2007, 2014). These studies were based on composite satellite imagery and classified landfast ice freeze-up through breakup over the whole Beaufort Sea region. Additionally, Johnson and Eicken (2016) found a trend of landfast ice breakup occurring 5 days earlier per decade between 1979 and 2013. Their study used satellite-derived sea ice concentrations to classify landfast ice breakup timing.

1.4 LANDFAST ICE MEASUREMENTS

A variety of techniques have been used to study sea ice and landfast ice in particular. These are primarily satellite imagery (Barry et al., 1979; Mahoney et al., 2006, 2007, 2014), in situ measurements from buoys, weather stations, and other sensors (Vaudry, 1987, 2006; Druckenmiller et al., 2009; Petrich et al., 2012) regional ice charts (Yu et al., 2014; Selyuzhenok et al., 2015), and local observations with radar and cameras (Druckenmiller et al., 2009; Petrich et al., 2012; Jones et al., 2016). Each technique provides a slightly different view of the landfast ice seasonal cycle and each has benefits and limitations.

1.4.1 *Satellite measurements of Landfast Ice and Ice Charts*

Satellite mapping of arctic sea ice began shortly after the first satellites were developed in the early 1960s (Wadhams, 2002). Initially, satellites were very low resolution, could not penetrate cloud cover, and were simply aerial photographs of the Earth from space (Wadhams, 2002). Depending on the satellite orbit and recorded swath size (the width of the captured images), the Arctic can be covered from every day to once every 20 days (Eicken et al., 2009; Wadhams, 2000). To study landfast ice cycle characteristics, from formation through breakup, high-resolution narrow swath area satellite images are needed.

In early studies of landfast ice along the Beaufort Sea LANDSAT imagery was analyzed. These images had a resolution of approximately 80 m and repeated sections of the Arctic Ocean about every 18 days (Barry et al., 1979). This satellite used a multispectral scanner (MSS) combined with visual cameras (Barry et al., 1979; https://landsat.gsfc.nasa.gov/the-multispectral-scanner-system/; https://landsat.usgs.gov/landsat-2-history). More recent studies have taken advantage of newer technology and different types of satellite measuring techniques. Synthetic Aperature Radar (SAR) is now the primary satellite class used to measure landfast ice extent and detect ice motion (Eicken et al., 2009). SAR provides narrow swath of about 100km and high-resolution images in all weather conditions, day and night (Eicken et al., 2009). Mahoney et al. (2005) outline using RADARSAT, a type of SAR with an infrared radar band, to detect sea ice. Images of the Beaufort Sea coastline taken every ten days are compiled together in mosaic images to yield a regional picture of the ice. Infrared imaging allows radar to see through the cloud cover, which is a frequent feature of the Arctic region.

This method of defining landfast ice breakup requires compiling mosaics of regional satellite images and comparing the images to detect motion in the landfast ice. From the RADARSAT images, ice motion can be detected by changes in the backscatter. However, as noted by Mahoney (2005), other factors affect backscatter besides ice motion, which can make motion detection in ice challenging. Frost flowers that form on the sea ice surface and changes in salinity are just two examples of ice properties that affect the backscatter. Another challenge in defining landfast ice breakup by this method is the combining of images from multiple days together over a period of $\pm$10–20 days (Barry et al., 1979; Mahoney et al., 2005, 2007). The combining of images to form the mosaic decreases the precision of event timing for landfast ice

formation, stable ice, breakup, and ice-free coast to ±10–20 days. The date range depends on how often the satellite passes over the regions of interested and records images for compilation.

Other studies of arctic landfast ice have used ice charts to characterize changes in the landfast ice season (Yu et al., 2014; Selyuzhenok et al., 2015). We mention this briefly here because satellite infrared and visible band imagery, shipboard and airborne observations, and local radar (Yu et al., 2014) are used to develop ice charts. U.S. National Ice Center (NIC) ice charts are published weekly and contain ice thickness, extent, and landfast ice. The charts provide a composite of ice data from the past week and not a snapshot image. It is important to note that ice charts do not show real-time data for landfast ice, as they are typically up to two weeks old given the satellite coverage timing. However, to examine changing conditions over the entire Arctic as in Yu et al. (2014), they are a very useful consolidated data set.

1.4.2 *In Situ Measurements of Landfast Ice*

Another common technique for measuring landfast ice breakup is to deploy buoys directly onto the ice and track their movement. Vaudry (1987) used several buoy deployments along the Beaufort Sea coast to follow the movement of ice during freeze up of the landfast ice, tracking winter storm events, and defining a breakup period when buoys floated freely. Newer buoys with GPS positioning systems allow precise tracking of ice movement over the period of position reporting. In the 1985–1986 study by Vaudry (1987) buoys only reported their positions daily.

In a report tracking multi-year ice flows and concentration, Vaudry (2006) used a variety of buoy types with either ARGOS or Nimbus RAMS to report hourly positions to a satellite. The precision on the variety of buoys used by Vaudry (2006) ranged from 350m to 2000m. This

multi-year ice study compiled a variety of buoy position data available from previous studies to come up with prediction table and the probability of ice movement in their defined seasons over the mid- to late 1980s (1985–1989). Using hourly positions from buoys deployed on landfast ice allowed detection of smaller scale ice motions and the ability to track effects of individual storm events. The report by Vaudry (2006) categorized landfast ice motion into bins of 0.2-knot motion speeds. Using buoys deployed onto fast ice can result in a very accurate measure of ice motion.

The accuracy of position tracking systems has improved since the data provided by buoys in the 1980s. The SVP buoys used in our study employ GPS technology to report their hourly positions. The accuracy of these buoys is within $\pm$ 4.0 m. The improvement in hourly position accuracy allows for a more precise measure of ice motion and start of the landfast ice breakup.

In addition to GPS tracking of ice location through buoy deployments on ice, investigators have deployed sensors to measure air temperature, air pressure, snow depth, ice thickness, and wind speed on the landfast ice. These in situ measurements of atmospheric and ice conditions provide data to compare with ice motion from GPS positions. A complete picture of the factors affecting ice motion can be determined.

The limitation to buoy and in situ measurement of atmospheric and ice conditions is the challenge of placing these sensors. Much of the Alaska Beaufort Sea coast is remote and difficult to reach to deploy ice buoys and weather sensors. Additionally, polar bears or other wildlife represent hazards for buoys and weather stations deployed on the landfast ice.

Typically, along the northern Alaska coast buoys and sensors are deployed once per year. Data from the SVP buoys are recorded in near real time and monitored for completeness. However because of remoteness and severe weather of this region, any stoppage in data recording cannot be fixed. Also using buoys versus satellite imagery only shows the ice motion at one or two locations. In contrast, satellite imagery is relatively inexpensive to view landfast ice along the whole Beaufort Sea coast.

Chapter 2. DATA AND METHODS

In this chapter, we will describe the data used for analysis of landfast ice breakup and forcing parameters affecting the breakup. Between 2007 and 2015 SVP buoys were deployed in two landfast ice lines, one each in Camden Bay and Harrison Bay. These SVP buoys report hourly GPS position signals, air pressure and air temperature. Additionally, we compiled data from the NARR NCEP reanalysis for air temperature and wind component velocities, water depths from a NOAA online chart viewer and water level from a NOAA tide gauge. In this study we first explain how the start of breakup is determined at each buoy location. Then we compare the ice velocity with wind speed to verify the buoy motion as ice movement. Next, we use several methods including visual analysis, correlations, and empirical orthogonal function analysis to make connections between the ice movement and other variables. Finally, we calculate the onset of thaw date and compare these results with previous observations of the region.

2.1 DESCRIPTION OF SVP BUOYS AND DEPLOYMENT

As part of the U.S. Interagency Arctic Buoy Program (USIABP), SVP buoys were deployed on landfast ice between 2007 and 2015. These SVP buoys aid in understanding conditions in the Beaufort Sea before breakup processes begin through the open water season. SVP buoys are spherical Lagrangian float buoys 35 cm in diameter (Figure 2-1) that report hourly GPS signals. Additionally, there are pressure and temperature sensors to measure air temperature and air pressure. These buoys were deployed on the landfast ice where they sat on the snow/ice and moved with the ice until it melted around them or fell into an open lead. The buoys then floated freely acting as a Lagrangian drifters with the surface currents and winds.

Figure 2-1 SVP ball buoy resting on landfast ice.

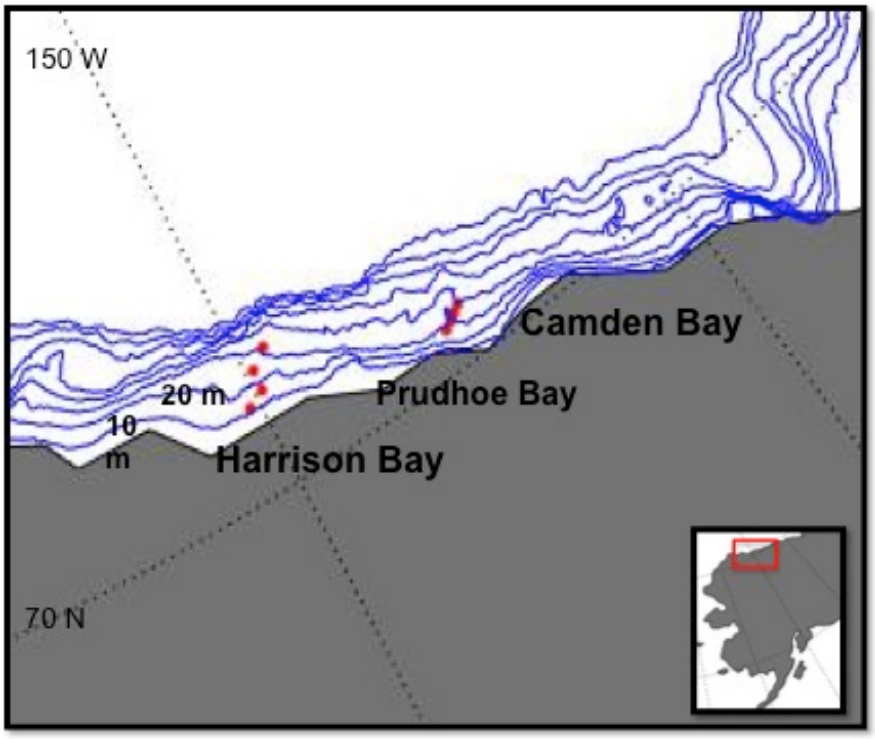

Figure 2-2 Deployment locations of landfast buoy line in Camden Bay to the east and Harrison Bay to the west. Bathymetry lines show in blue at 10, 20, 30, 40, 50, 100, 250, and 500 m.

Repeated landfast ice lines of SVP buoys were deployed from 2010 to 2015, with slightly different deployment locations in 2007–2009 (Figure 2-2, Tables 2-1 and 2-2). The buoys were deployed on the fast ice typically in late January, February or March each year. Before being deployed the areas were inspected to ensure landfast ice was indeed fast to the shore and not drifting. Due to the highly deformed nature of landfast ice in this region, the deployment location of buoys was not the same year to year, but as close as possible. Flat, stable landfast ice was found for deployments.

In each year of our study between six and eight SVP buoys (Tables 2-1 and 2-2) were deployed on landfast ice at two locations, Camden Bay to the east and Harrison Bay to the west (Figure 2-2). In Camden Bay the buoys were deployed between 13 km and 40 km from shore, except in 2008 and 2015, when one additional buoy was deployed 8 km from shore. In Harrison Bay they were deployed between 13 km and 52 km from shore, except in 2007 when one buoy was deployed near the mouth of the Colville River delta. The disparity in these distances is because the average SLIE extent and 20-m isobaths extend farther from shore in Harrison Bay than Camden Bay (Figure 1-4 and Figure 2-2). In Camden Bay, the buoys were each spaced 6–7 km apart along the line. In Harrison Bay the A-C buoys were spaced approximately 16–17 km apart; in the two years D buoys were deployed they were approximately 10 km from the C buoy. In Harrison Bay the average extent of landfast ice is 50 km from shore. These buoys were placed in snow on the landfast ice and remained on the ice tracking its position until it melted away, and the buoy floated freely.

Table 2-1 Camden Bay Buoy Deployments and Breakup Date

Beacon Year	Buoy Abbrev.	Deploy Date	Deploy Latitude	Deploy Longitude	Approximate Depth (m)	Breakup Date
2007	CB-1	1/25/07	70.26520	-145.93539	18	7/4/07
2007	CB-2	1/25/07	70.29900	-145.76241	25	6/8/07
2007	CB-3	1/25/07	70.36580	-145.59520	29	7/5/07
2007	CB-0	2/22/07	70.24860	-146.18340	12	6/29/07
2008	CB-1	2/5/08	70.28360	-145.92841	21	4/21/08
2008	CB-2	2/5/08	70.30000	-145.75420	25	4/20/08
2008	CB-3	2/5/08	70.37600	-145.57179	30	4/2/08
2008	CB-4	2/5/08	70.39860	-145.37460	35	4/3/08
2009	CB-1(2)	3/21/09	70.26920	-145.95180	18	5/17/09
2009	CB-2(2)	3/21/09	70.31680	-145.70480	26	5/17/09
2009	CB-3(2)	3/21/09	70.37520	-145.55161	32	5/17/09
2009	CB-4(2)	3/21/09	70.39220	-145.29700	35	5/17/09
2010	CB-1	1/12/10	70.26876	-145.92672	18	8/5/10
2010	CB-2	1/12/10	70.29882	-145.91700	21	7/5/10
2010	CB-3	1/12/10	70.35948	-145.58022	30	7/6/10
2010	CB-3(2)	4/4/10	70.36902	-145.58004	32	6/28/10
2010	CB-4(2)	4/4/10	70.40286	-145.36044	34	7/1/10
2011	CB-3	1/27/11	70.36640	-145.57300	30	6/17/11
2012	CB-1	1/26/12	70.29860	-145.64980	24	6/19/12
2012	CB-2	1/26/12	70.33340	-145.46120	29	5/15/12
2012	CB-3	1/26/12	70.36440	-145.32120	31	6/18/12
2012	CB-4	1/26/12	70.40000	-145.14060	36	6/18/12
2013	CB-1	2/2/13	70.30500	-145.86760	22	5/14/13
2013	CB-2	2/2/13	70.33100	-145.73360	25	5/15/13
2013	CB-4	2/2/13	70.40080	-145.39540	33	3/5/13
2014	CB-1	2/25/14	70.31800	-145.84700	24	5/2/14
2014	CB-2	2/25/14	70.32900	-145.71500	26	5/2/14
2015	CB-00	2/25/15	70.23480	-146.12920	7	6/25/15
2015	CB-0	2/25/15	70.27500	-145.99300	15	6/9/15
2015	CB-4	2/25/15	70.40100	-145.41500	34	4/22/15

Table 2-2 Harrison Bay Buoy Deployments and Breakup Date

Beacon Year	Buoy Abbrev.	Deploy Date	Deploy Latitude	Deploy Longitude	Approximate Depth (m)	Breakup Date
2007	HB-A	2/22/07	70.50660	-150.50501	1	7/11/07
2010	HB-A	4/4/10	70.63542	-149.83506	9	7/7/10
2010	HB-B	4/4/10	70.75206	-149.77584	16	7/5/10
2010	HB-C	4/4/10	70.85502	-149.73588	19	7/5/10
2012	HB-A	1/27/12	70.63160	-150.24840	12	7/4/12
2012	HB-B	1/27/12	70.69940	-149.83200	15	6/29/12
2012	HB-C	1/27/12	70.84980	-149.80260	17	7/2/12
2013	HB-A	2/3/13	70.63200	-149.83660	9	7/7/13
2013	HB-B	2/3/13	70.70080	-149.43300	10	7/8/13
2014	HB-A	2/26/14	70.62400	-149.82400	9	7/3/14
2014	HB-B	2/26/14	70.70500	-149.42100	10	6/30/14
2014	HB-D	2/26/14	70.94500	-149.37200	22	5/2/14
2015	HB-A	2/25/15	70.62500	-149.83200	9	6/23/15
2015	HB-B	2/25/15	70.70700	-149.40600	19	6/23/15
2015	HB-D	2/25/15	70.95400	-149.36700	22	6/30/15

Data from these buoys were analyzed for completeness of the time series and length to ensure that they captured landfast ice breakup. All data time series that did not show any movement or ended before April of the year they were deployed were discarded. Without showing any movement, the buoy data were not usable to determine ice breakup. There were ten buoys eliminated from the data analysis because their time series were too short to show movement. Additionally, data at the beginning of each time series captured testing of the buoys before deployment on landfast ice and travel to the deployment locations. Time series were cut to eliminate these data, based on the GPS position of the buoy and distance traveled in an hour.

The SVP buoys report hourly GPS positions, but, some of the records have gaps. Gaps were examined for the length of missing data and the position of the buoy before and after the gap. If there were gaps in the time series where the buoy traveled a distance greater than 10 km

or the gap was longer than five days the time series was discarded. These criteria resulted in five of the remaining 49 buoys being discarded. Tables 2-1 and 2-2 show the list of buoys used to calculate breakup in each year. For the remaining time series where there were short data gaps, the hourly positions were interpolated linearly. This approach used the latitude and longitude before and after the gap to linearly interpolate the position. Most of the gaps in the time series were about two to five hours long and during periods when the location of the buoys was the same before and after the gap.

Additionally, NOAA online electronic charts for the Alaskan coast were used to find approximate water depths at each buoy deployment location. The charted depths were used to compare depth of water at the deployment location for each buoy with ice breakup timing. Depths were estimated to the nearest meter unless the charted position fell directly over a data point. We classify this case as an estimated depth because the bathymetry in the area along the Beaufort Sea coast of Alaska is not well mapped. These data are used to examine the link between water depth and timing of landfast ice breakup.

2.2 FORCING PARAMETER DATA

To classify the breakup each year as mechanical or thermal, we examine the effects of surface winds, air pressure, tidal heights, and surface air temperature on ice movement. Previously published studies have also used current velocity to classify breakup mechanisms, but due to a lack of current measurements in the region over the time span of our study, this approach was not possible for this study. Air pressure data used in this analysis were recorded hourly on the SVP buoys. The SVP buoys also record air temperature; however, these data were not used in our

analysis because buoys tend to roll over, exposing the temperature sensor to increased solar heating and thus inaccurate air temperature measurements.

2.2.1 *Air Temperature and Wind Velocity Data*

Air temperature and the meridional *(u)* and zonal *(v)* components of wind velocity are from the NARR NCEP reanalysis data provided by the NOAA/OAR/ESRL PSD (Boulder, Colorado http://www.esrl.noaa.gov/psd/). These data are in 8x daily increments, or 3 hourly means of air temperature and *u* and *v* wind velocity components. We used two data points, one in each bay region, from the 2-m air temperature and 975-mb level wind velocity data sets. The level of these data were chosen for our analysis instead of surface air temperature and surface wind velocities to eliminate effects of turbulent interactions with the surface. Data from February 1 through September 30 each year from 2007 to 2015 were downloaded for processing and correlation analysis with buoy velocity. Air temperature and wind velocity components from the closest data point to landfast ice lines in each bay were used for calculations.

2.2.2 *Air Pressure Data*

Surface air pressure measurements were taken from the time series data reported by SVP buoys. As with the positions where there were gaps in the received buoy data, air pressure was linearly interpolated. The interpolation method produced a linear interpolation of missing air pressure values based on the trend of air pressure before and after gaps. Air pressure is reported in mb and is measured at the top of the buoy approximately 1 m above the surface at the top of the buoy.

2.2.3 *Mean Tidal Height Data*

For the study of water movement under the landfast ice, we were limited to a NOAA tide gauge at Prudhoe Bay, AK (Figure 2-2). This sensor is the only year-round tide gauge that provides water level data near the land fast ice lines. The tide gauge is approximately half way between the Camden Bay fast ice line and the Harrison Bay fast ice line. Data from the NOAA Prudhoe Bay Station tide gauge for the period 2007–2015 were downloaded from https://tidesandcurrents.noaa.gov/stationhome.html?id=9497645. The tidal data are height above or below mean lower low water level every hour.

2.3 METHODS TO DETERMINE BREAKUP DATE

Once the quality control and completeness checks of the position time series were completed, we calculated the buoy velocity, which represents the speed of landfast ice. Speed is defined as distance divided by time. Knowing that the time step in our position data is 1 hour we needed to calculate the distance between each reported position. The distances between each latitude and longitude pair have been computed using the Haversine formula. First, the differences between latitude and longitude positions at each time step were calculated. Due to the $\pm$4.0 m accuracy in GPS positions, any distances below 8.0 m were set to zero. This correction accounted for the possibility that the latitude-longitude pair transmitted by the buoy could have been off by up to 8.0 m from the actual position of the buoy. The average latitude for the position of the buoys throughout the ice breakup season was 71 °N, which we used to calculate the radius of the Earth, to correct for a slightly smaller radius at higher latitudes. Component velocities of each buoy were calculated from the total velocity using the direction between each latitude and longitude time step pair. The direction for the velocity vector enabled the calculation of meridional, u, and zonal, v, components of the velocity at each hour time step.

For analysis of ice breakup, the speed, $(u^2+v^2)^{1/2}$, of the buoy was used, but we also calculated u and v components. Once the distance in meters was calculated between each reported position, it was divided by the time difference, 1 hour, or 86400 sec. An example of the velocity time series for one of the buoys can be seen in Figures 2-3 and 2-4. The velocity time series allows us to detect first movement of the ice and determine starting breakup date for each buoy location. We defined break up as 0.1 m s^{-1} and greater movement for one day without periods of zero velocity for longer than two days. This definition eliminated early movement detected in the ice that did not classify as complete breakup of landfast ice. Discussion of the resulting breakup start found from velocity profiles for each buoy are given in the next chapter.

Landfast ice breakup for this study is defined as the first day of consistently detectable buoy movement. We defined breakup in this way to rule out early movement events movement events that did not coincide with the melt season and coast becoming ice-free. In several years, buoys deployed furthest from shore showed, in water deeper than 25 m, early movement or break out events that lasted between several hours to a few days, but were not continuous through the spring and summer. Figure 2-5 shows one of these events, where the velocity time series of two buoys in 2010 showed spikes of movement between days 100 to 120. The ice moved consistently for a few days but reattached or grounded after a period of 10–15 days movement. In 2010 these two buoys show breakup occurring on day 185.

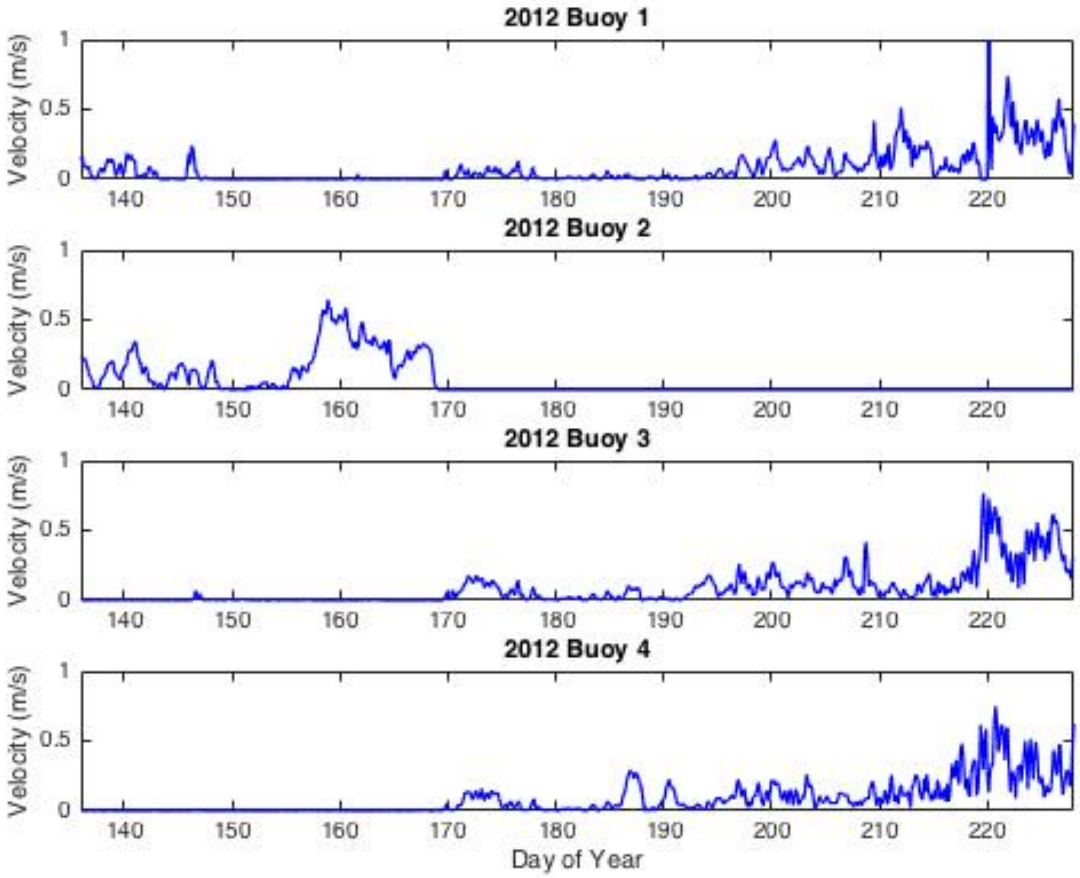

Figure 2-3 Sample of velocity profile time series from 2012 Camden Bay buoys. Buoy velocity is plotted against the day of year.

Each velocity time series was examined with the position of the buoy as it moved in time. If the buoy/ice moved within the bay region early in the season and reattached or grounded, as detected by 0.0 m s^{-1} buoy velocity within that same bay and remained stable for a length of time we did not classify it as breakup. We needed to see continuous motion or movement out of the bay to classify as breakup. The events early in spring during which the buoy showed detectable movement for greater than one day, but then became stable, are classified as breakout events.

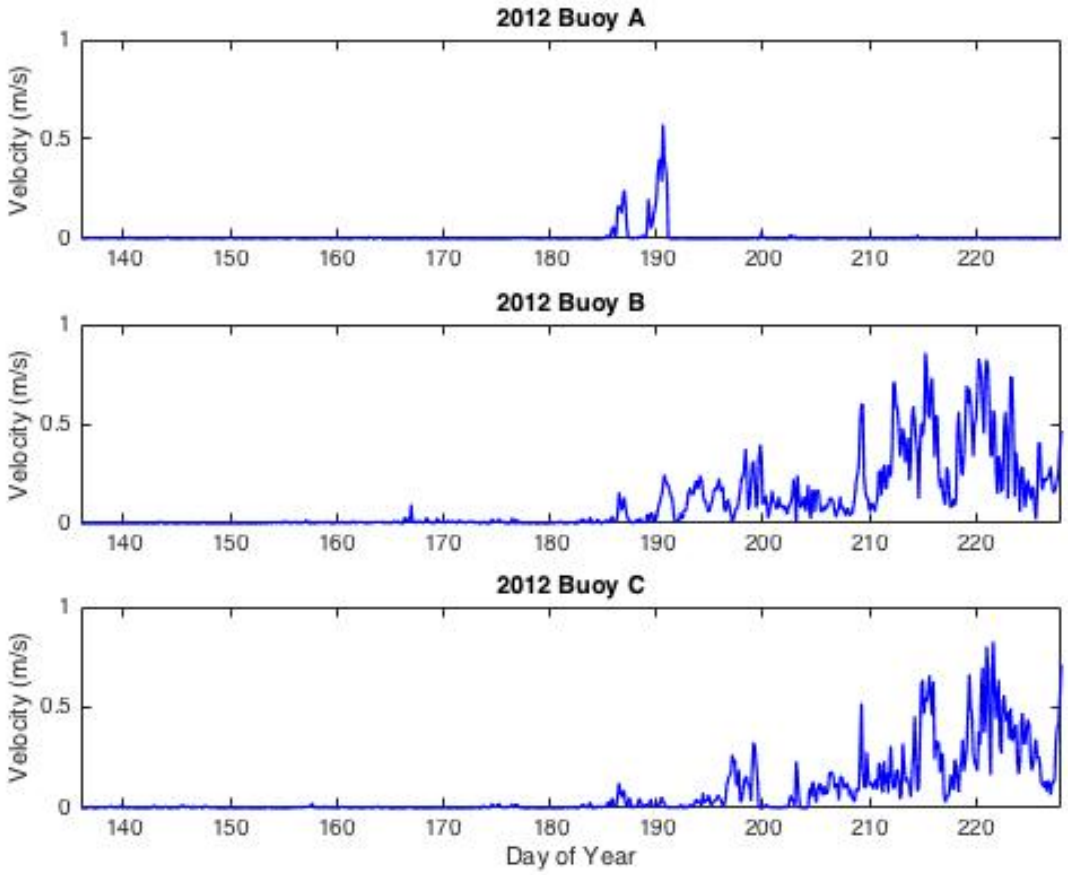

Figure 2-4 Sample of velocity profile time series from 2012 Harrison Bay buoys. Buoy velocity is plotted against the day of year.

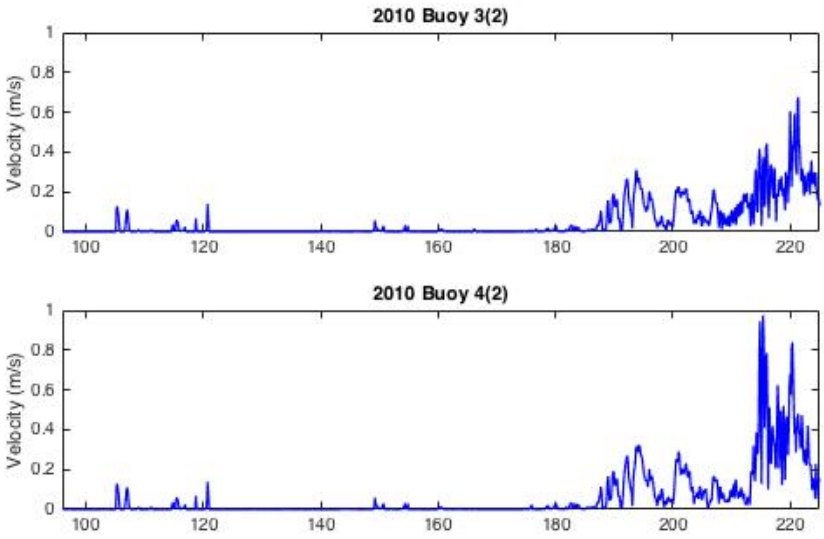

Figure 2-5 Velocity profiles for two buoys from Camden Bay showing early local movement events on yeardays 105–120, where the ice reattached and became landfast until a breakup occurred on yeardays 185.

As a further step to classify ice breakup, we compared the buoy velocity with wind speed. As a rule of thumb freely drifting sea ice will travel at 2% of wind speed. In the ice motion measurements from Camden Bay in 1985–1986 Vadury (1987) reports landfast ice to moving at 1–2% of the wind speed as it broke free. To classify the ice movement detected by buoy position as freely moving, we compare the velocity from the buoys with wind speed. The beginning buoy speed as a percentage of wind speed is discussed further in the next chapter.

2.4 METHODS TO ANALYZE FORCING PARAMETERS

The data provided by the NARR data sets are in 8x daily increments, which are 3 hourly means. To compare ice/buoy velocity, air pressure, and tidal height with the NARR wind and air temperature data, we needed to calculate 3 hourly means for these data sets. This averaging allowed for a direct comparison of all parameter data components at each 3-hour time step. Figures 3-5 and 3-6 show examples of time series for buoy velocities and the forcing parameters

over the time of ice breakup. A simple visual examination of these time series plots can show possible connections between the buoy movement and forcing variables.

2.4.1 *Linear Correlations*

As the first test of quantifying the relationship between the forcing parameters and buoy speed, we calculated the correlation for each year between each buoy time series and air pressure, air temperature, *u* and *v* wind components, and water level. The correlation between two variables is tested by the least squares fit. It is a simple test to determine whether or not the two data sets are related. Correlations between each buoy speed and each forcing parameter were calculated. Covariance provides a measure of the fraction of explained variance by a linear least square fit to total variance, in other words, how much the two variables change together.

Because we are trying to quantify which forcing parameter, or combination of parameters, causes the ice movement at breakup to occur, we cut each time series down to a section 75 days in length. We ensured that this time chunk for each year covered the start of the movement for all ice buoys; beginning 45 days before through 30 days after the average breakup day per year. Table 3-1 lists the correlation coefficients (*r*) between each buoy speed and each forcing parameter.

2.4.2 *Empirical Orthogonal Function Analysis*

Another common method for determining or explaining the variability of a data field to determine a set of "predictors" of variables is the empirical orthogonal function (EOF) method. This analysis method deconstructs a set of data into a new set of predictors, or modes, that explain the maximum amount of variance in the dependent sample. These new predictors are

orthogonal to each other. All of the modes that are returned from an EOF deconstruction account for the combined variance in the data set (Thomas & Emery, 2014). The key advantage of an EOF analysis is that it provides a way to view the temporal structure in our data that explains the most variance between variables. This structure can provide us with information about whether one forcing parameter dominates the variability in ice movement. In our deconstruction, we compared the variable structures (buoy speed, air temperature, wind speeds, air pressure, water level) with the temporal structure to see if a common temporal structure was present in the data. The exact method of deconstruction used is a principle component analysis (PCA) because the variables used were de-trended and normalized.

We ran two separate PCA analyses, one each for Harrison and Camden bays. Here we will outline how the data matrix for each PCA analysis was set up. First, the data were set up so that each variable had the same 3-hour time step corresponding with the NARR wind and air they were available from only one buoy. Additionally, because there were no buoys deployed in the Harrison Bay between 2008 and 2009 and only one in 2007, the Harrison Bay data matrix contains buoys from 2010, and 2012–2015. In each year two buoys, one near shore and one further offshore, were chosen for the PCA analysis because there were some years over the 8-year period that only had two good time series (see Tables 2-1 and 2-2). The period chosen for PCA analysis was April 1 00:00 thru July 31 21:00 for the Camden Bay analysis and April 6 00:00 thru July 31 21:00 for the Harrison Bay analysis. This shift of 5 days in the Harrison Bay analysis was due to the buoys in 2010 not being deployed until April 5. The data matrix for each region was set up so that the rows contained each variable and columns contained time steps. Variables for each year were stacked in the rows, so that the matrix contained each variable from

April to July with 2007 as the first X rows, then 2008, then all the way to 2015. Stacking all of the data together allowed us to look for an overarching structure to the variability of ice movement and forcing parameters over the course of the whole study period.

Before deconstructing our data using the PCA method, we had to detrend and normalize the data. The data matrix, however, contained variables with different units and orders of magnitude — m s^{-1}, °C, mb, and m. An EOF analysis could be run on data set before detrending and normalizing, but results could have been skewed by the numerical difference of three orders of magnitude between air pressure and buoy velocity. The mean of each variable was subtracted from the individual data points for that variable in the time series. This step removed the trend from each variable time series. Additionally, this calculation brings the variables, which had different units and orders of magnitude, closer together in size. The next step to compare the variable in a deconstruction method, without skewing the results towards the largest or smallest order of magnitude, was to normalize the data by dividing each variable by its standard deviation.

The PCA method is a deconstruction tool that finds the dominant modes of the combined variables in our time series. PCA deconstructed the data matrix into rank-ordered modes in time and among our variables, ordered such that the first mode explains the most variance among the data, the second the second most explained variance and so on. In our analysis we computed two PCA deconstructions, using data for each of the two fast ice buoy lines with forcing variable data.

2.4.3 *Onset of Thawing Temperature*

Another frequently used classification of ice breakup timing is to compare it to the days after melt onset (Barry et al., 1979; Mahoney et al., 2007, 2014; Petrich et al., 2012). To calculate onset of melt we calculated a two-week running mean of the 2-m air temperature. We defined onset of thaw as the first day where temperatures rise above –1.0 °C and where that day coincides with the start of a two-week period where the average daily temperature was above –1.0 °C. Taking the running mean of our temperature time series with a window length of 14 days gives the 2-week period average daily temperatures. From the running mean temperature we were able to determine when air temperature passed above –1.0 °C (Figure 2-6). In Table 3-2 we list the onset of thaw date for each year when the mean regional air temperature was used and specific dates for Camden Bay and Harrison Bay. We chose –1.0 °C to quantify the start of melt because of sea ice parameters that allow it to begin melting before reaching 0.0 °C, consistent with methods used by Rigor et al. (2000).

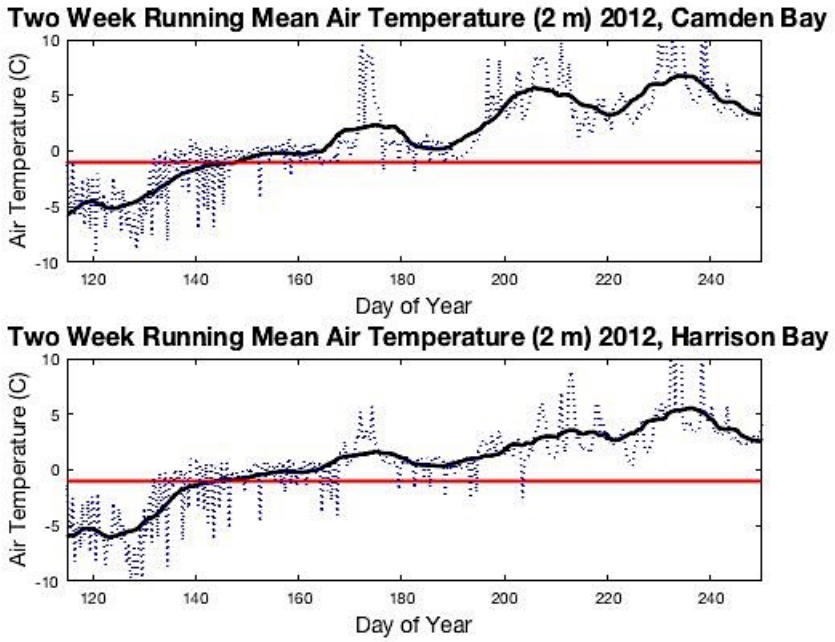

Figure 2-6 Sample of air temperature time series used to calculate the onset of thaw each year. Top figure air temperature from Camden Bay, bottom figure air temperature from Harrison Bay. Black line two week running mean air temperature dotted blue unsmoothed air temperature, and red line shows –1.0 °C.

Chapter 3. RESULTS AND DISCUSSION

In this Chapter, we present our results and seek to explain the conditions of landfast ice breakup during the period of our study. The breakup timing over the study period of 2007–2015 is in agreement with results reported by Mahoney et al. (2014), with an average start date of June 6. This date is 24 days earlier than the beginning of breakup over the period of 1973–1977 reported by Barry et al. (1979). Harrison Bay has very consistent breakup timing from year to year, and Camden Bay has greater variability. Examining the possible forcing variables affecting the timing of breakup we found that in Harrison Bay ice did not move until an average of 35 days after the onset of thaw. In Camden Bay, ice movement began only after five thawing days. PCA analysis did not provide robust covariance between the buoys and forcing parameters. Additionally, correlation coefficients were low, but some patterns arose where breakup in years was strongly correlated with zonal winds. Overall we classified breakup as thermal for each year in Harrison Bay and mechanical for five out of the nine years in Camden Bay.

3.1 Breakup Timing Results

Examining all buoy positions and movement over time during the late spring and summer each year shows that the landfast ice broke free at different times in the east and west. These results are in agreement with observations reported by previous studies of the Beaufort Sea coast (Vaudry 2006; Mahoney et al., 2014). To better understand the dynamics in this region we examine the ice breakup over the whole region and in the two bays (east and west regions) separately.

The buoy velocity time series and maps with hourly positions plotted allowed us to identify the onset of break up began accurately. A sampling of buoy velocity time series (Figures 2-3 and 2-4) shows that in some years the ice moves slightly throughout the season and other years the ice remains motionless until break up occurs. To ensure correct pinpointing of the start of breakup, the positions of the early movement periods were examined. We classified break out events by examining a combination of the buoy's hourly positions on a map (Figure 3-1) and the velocity time series (Figures 3-2) we classified break out events. This approach led us to determine when velocity peaks resulted in the buoy moving within the local bay and re-grounding or freezing or when the buoy/ice broke free and drifted out of the area. These early ice movements, or break out events, were more common in Camden Bay.

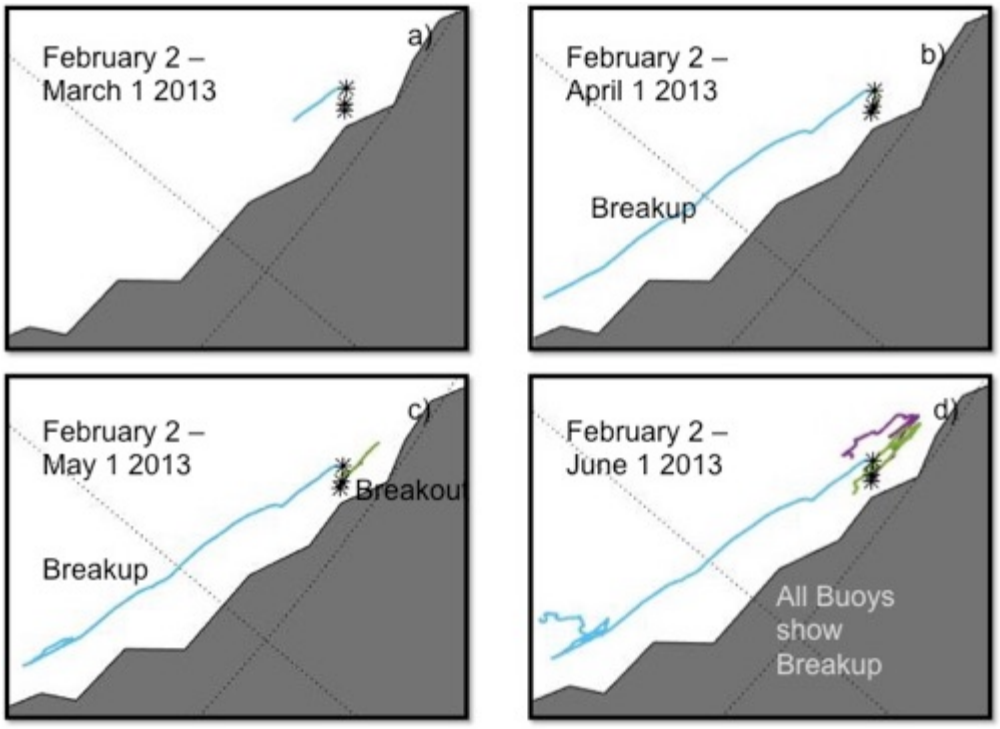

Figure 3-1 Sample buoy track from February–June 2013 comparing break out events with breakup. The black stars are starting positions for each buoy deployed in Camden Bay. a) Buoy farthest offshore began continuous movement, showing breakup. b) and c) show break out events that were not continuous and did not result in buoys moving out of Camden Bay.

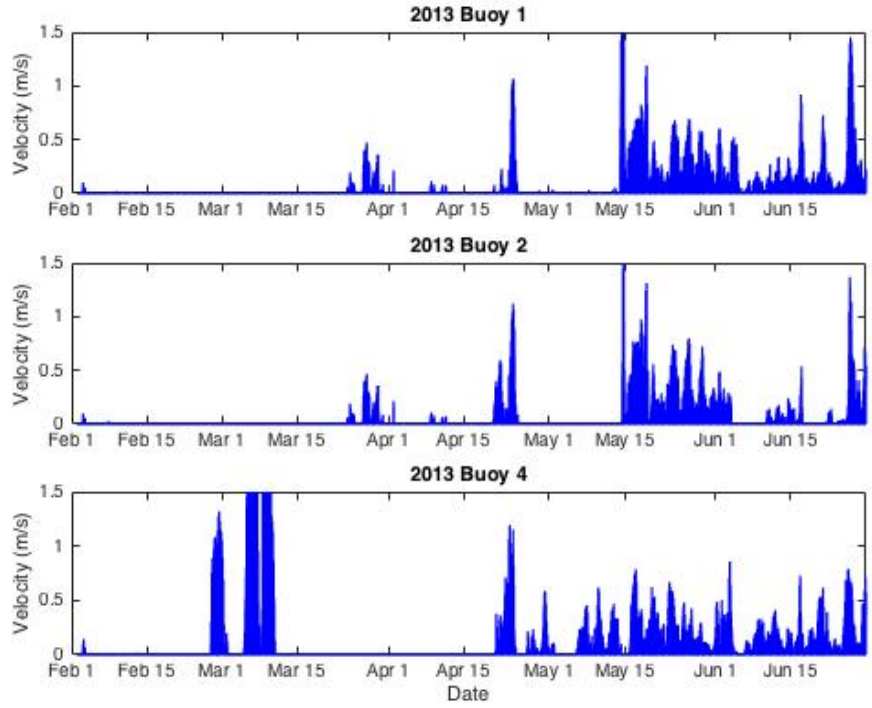

Figure 3-2 Sample of velocity time series for 2013 Camden Bay buoys. Early movement (April) in buoy 1 and 2 are break out events. Movement in buoy 4 shows break up starting in March.

These early breakouts are common occurrences (Barry et al., 1979; Vaudry, 1987; Mahoney et al., 2007, 2014), and were not considered breakup for the individual buoys that moved unless the ice did not appear to reattach or ground somewhere else in the region. Additionally, these dates were not used in the individual bay studies but only in calculating the regional mean. For example, in 2008 the buoys deployed farthest from shore in Camden Bay broke free on the day of year 94 and 93 and remained in motion through the end of the summer. We used these breakup dates in the Camden Bay mean calculation. However, in 2007 the two buoys farthest from shore began moving from the Camden Bay region on yeardays 43 and 45 but then became stable again further to the west, past Prudhoe Bay, and remained mostly stable until

yeardays 159 and 180. These later dates were used in the overall regional mean break-up date, but the earlier dates were not used in the Camden Bay breakup mean.

Figures 3-3 and 3-4 show breakup timing averaged over the whole North Slope region and separated out into the two different bays. The error bars represent one standard deviation from the mean breakup day. In both Figures 3-2 and 3-3, the error bars for certain years are quite large because of the sometimes month or longer differences in breakup timing between the two regions and because within each Bay region per year there were only 2–5 buoys. The small sample size led to a large standard deviation when a disparity between buoys closer to shore and farther offshore began moving at different times. We also observed a large amount of variability from year to year, especially within the Camden Bays data (Table 2-1). In Harrison Bay, there was greater consistency in date of movement across the fast ice line (Table 2-2). Whereas in Camden Bay we observed earlier buoy movement in those deployed farthest from shore.

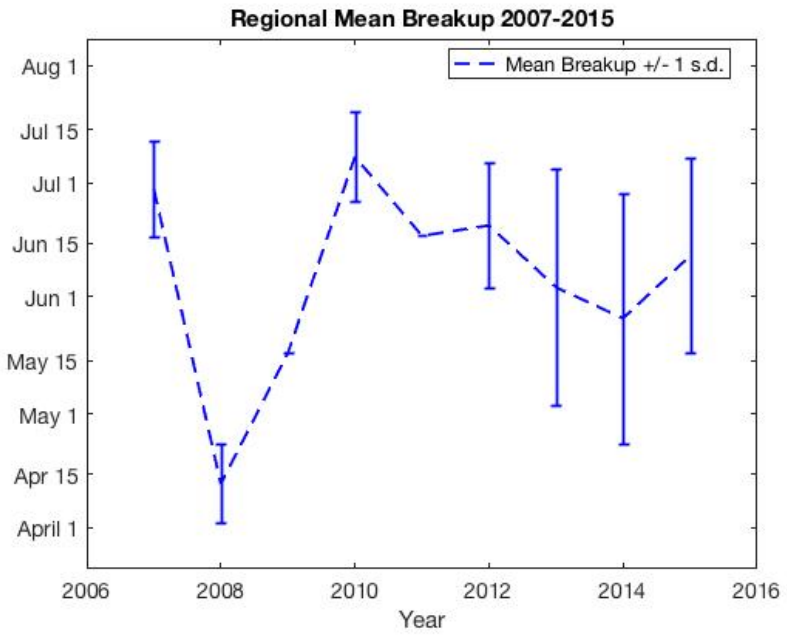

Figure 3-3 Mean breakup date for each year of the study period. Error bars show +/- one standard deviation from the mean.

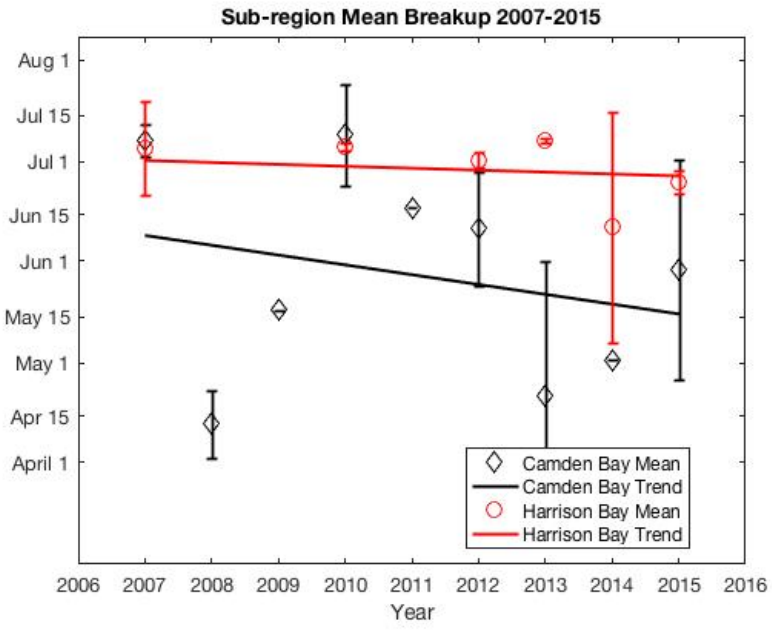

Figure 3-4 Mean breakup date per year separated by study area. Red markers are the mean breakup date each year where there were available data for Harrison Bay. Black markers are the mean breakup date each year where there were available data for Camden Bay. The lines (red Harrison Bay, black Camden Bay) are overall trends of the breakup timing 2007–2015.

3.2 Discussion of Breakup Timing

The mean breakup day was calculated from the time that each buoy began moving continuously. The regional average over the 9-year period was calculated so that our results could be compared with previous studies. The average breakup for the Beaufort Sea coast during 1973–1977 started on June 30 (Barry et al., 1979), and during 1996–2008 breakup began on June 11 (Mahoney et al., 2014). We report the average breakup day during 2007–2015 to start on June 6. We found the start of landfast ice breakup to occur 24 days earlier than in the 1970s (Barry et al., 1979). This trend is not statistically significantly different from the breakup start date reported by Barry et al. (1979), but it does show a continuing trend of earlier land fast ice breakup in the Beaufort

Sea region. Additionally, our results showed the landfast ice breakup to start 5 days earlier than during 1996–2008 (Mahoney et al., 2014), which was also not statistically significant. These previous studies used satellite imagery to calculate start of breakup, and thus have a ± 10–15-day error. The trend we report for 2007 and 2015 shows an average earlier breakup of about half a day per year.

Next, we examined differences in the breakup date for the east region, represented by the Camden Bay line, and west region, represented by the Harrison Bay line. The timing of the start of breakup among the Camden Bay buoys showed greater variability than the Harrison Bay buoys. Figure 3-3 shows the ± 1 standard deviation for Harrison Bay had a smaller range from year to year than the Camden Bay buoys. Additionally, Table 2-2 shows the breakup dates for Harrison Bay are very consistent; throughout most years the buoys all began moving on the same day of the year. In Camden Bay, there were certain years, 2008, 2012, and 2015 for example, when one or two of the buoys began moving much earlier than others (Table 2-1). The breakup date for Camden Bay has a larger range for the ±1 standard deviation (Figure 3-3). Despite these differences in the breakup date between the two regions, the buoy data did show an overall trend towards earlier landfast ice breakup. In Camden Bay, the trend to earlier breakup was larger than Harrison Bay, almost four days earlier per year for the former, and nearly two days per year earlier for the latter.

Further analysis (Figure 3-3) shows that although the overall trend shows earlier breakup, year to year there was a large amount of variability. This variability combined with the differences in breakup date in each bay motivated us to study the factors dominating the breakup

year to year, and their key differences in years of extremely early or late breakup. Past studies in this region of landfast ice state that thermodynamic processes dominate the forces causing breakup. However, a recent study of landfast ice breakup off Barrow, AK (Petrich et al. 2012), reports a trend towards increased mechanical processes acting to break out the landfast ice before thawing temperatures cause the ice to melt or decay enough to break free. Our analysis sought to determine if there is a similar trend along the Beaufort Sea coast region. With landfast ice buoy lines in two Beaufort Sea regions, and different breakup patterns and timing, we sought to identify forcing factors affecting the start of breakup in each bay.

One limitation in using buoy only buoy data to classify breakup is not having a picture of the whole region and what may have caused some of the early break-out events. Satellite data or radar observations of the landfast ice, as used in previous studies, can show when pack ice impinges and breaks off a portion of the seaward edges of the landfast ice. With our data set, we were limited to plotting the buoy positions, velocity time series, and comparisons with weather and tidal data for clues to events causing motion in parts of the landfast ice line.

3.3 Forces Affecting Breakup

To answer why breakup was earlier in some years than others, and why there was a difference in timing between two different bays along the same coastline approximately 150 km apart, we considered the main driving forces that cause landfast ice breakup. Landfast ice breakup is either thermal, where the ice stays fast to the shore until it melts in place after enough energy input from above freezing temperatures, or mechanical, where it is forced by wind stress, high water

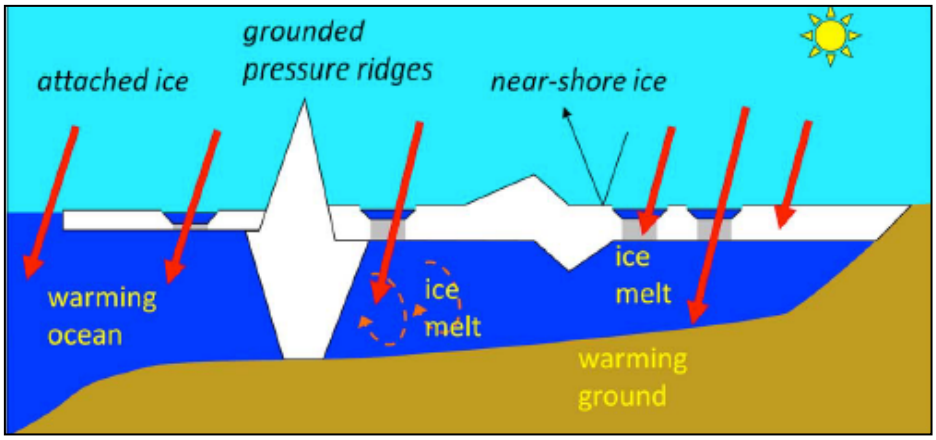

Figure 3-5 Schematic (Petrich et al., 2012) showing thermal penetration affecting ice breakup during late spring/early summer near Barrow, AK.

levels, or strong currents, to break free from the coast and unground keels. Ice can melt in place when thermal radiation acts to both melt the surface landfast ice and warm the waters around keels to melt them (Figure 3-5). With changing conditions in the Arctic, i.e., increased open water season leading to increased warming, less multi-year pack ice, and the trend towards thinner first-year ice, do mechanical processes break up landfast ice earlier than thermal processes?

We compared the time series of buoy velocity with time series of the forcing parameters — water level, air pressure, air temperature, wind speed, and direction. A time series for the month before and after breakup from Camden Bay in 2007 (Figure 3-6) shows a time of higher air pressure about ten days before the detection of ice motion. Also, the temperature is consistently above the –1.0 ℃ thawing temperature of sea ice during the month before breakup. Finally, there is a shift in wind with slightly higher than normal wind speed, but not as different from

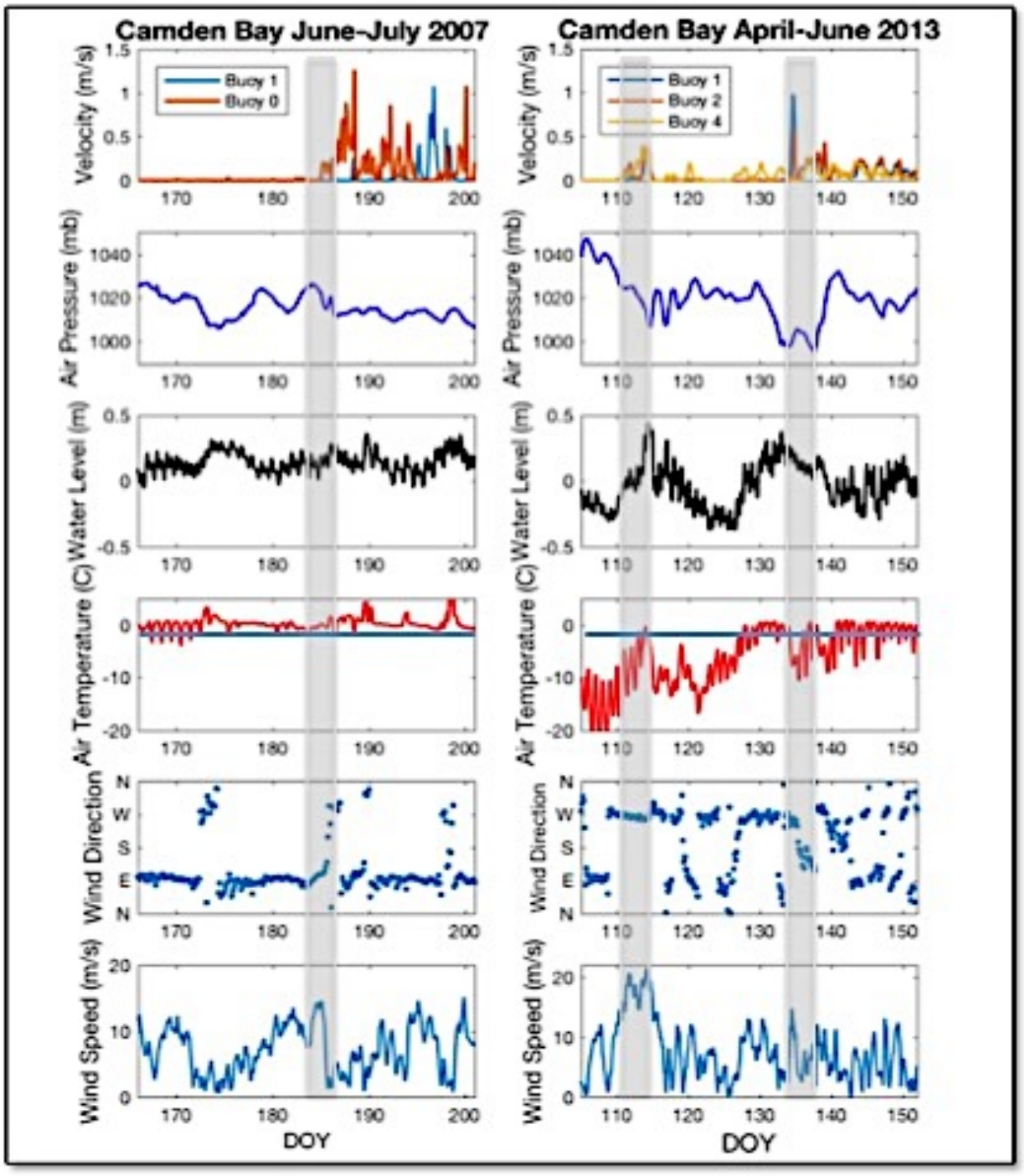

Figure 3-6 Camden Bay buoy velocities compared with time series of forcing parameters; 2007 is on the left and 2013 is on the right. Gray shaded areas highlight days buoys showed breakup. Horizontal line in the temperature time series shows melting point for seawater, –1.0 °C. Note the time series yeardays differ between 2007 and 2013; each shows the month before breakup through 15 days after breakup started.

average wind speed as is seen during other movement events. Camden Bay in 2007 is classified as thermal breakup because there is no clear indication of mechanical forcing, and breakup started well after the onset of thaw.

In 2013 in Camden Bay it is clearer that early buoy movements around yearday 110–115 coincide with weather and sea level events (Figure 3-6). Around this time air pressure dropped by about 40 mb, water level above the mean lower low water level rose by about 0.5 m and wind speeds were above 20 m s^{-1} out of the west. The most likely reason ice moved this early in the season was a storm event. Additionally, when the landfast ice broke up and moved out of the Camden Bay region around yearday 135, there was a concurrent air pressure decrease, and increase of the water level and winds out of the west, though not as strong as the earlier event. Camden Bay in 2012 is classified as a mechanical breakup year.

In Harrison Bay in 2010 (Figure 3-7) the buoys remained very stable until breakup. The water level above mean lower low water reference level increased by 0.1–0.2 m before the breakup, with greater daily amplitude between high and low water levels. These data align visually with the start of buoy movement, but they could be explained by the region around the pressure sensor becoming ice-free and thus allowing for slightly higher tides without the damping effect of sea ice. The temperature profile shows that air temperatures begin to remain at or above the thaw threshold for sea ice for the ~ 30 days before buoy movement begins. Because temperatures were such that would cause thawing, we classified Harrison Bay in 2010 as thermal breakup.

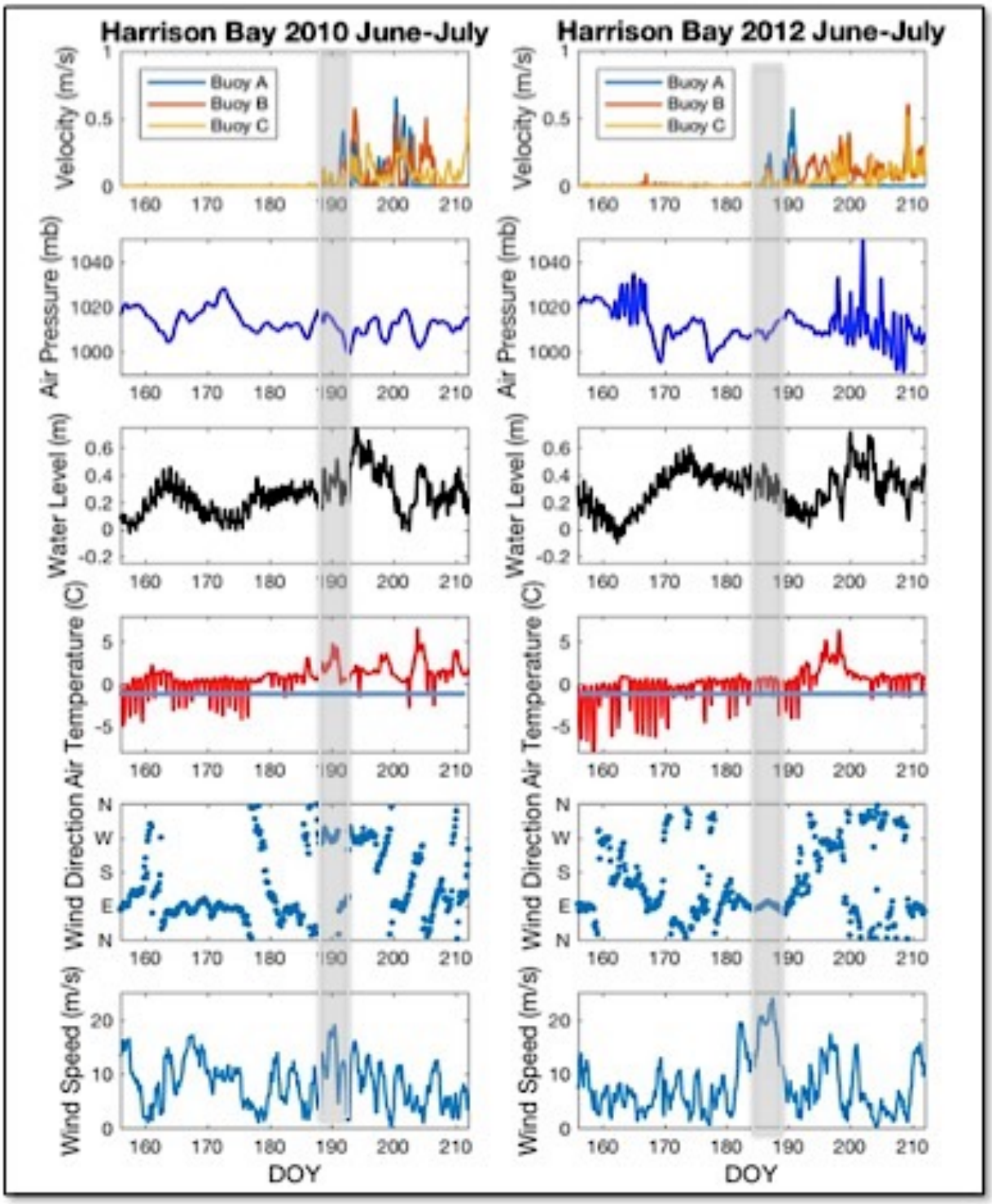

Figure 3-7 Harrison Bay buoy velocities compared with time series of forcing parameters; 2010 is on the left and 2012 is on the right. Gray shaded areas highlight days buoys showed breakup. Horizontal line in the temperature time series shows melting point for seawater, –1.0 °C.

In Harrison Bay in 2012 buoy movements appears correlated with ice motion during a nearly 10- day period of easterly winds consistently above 15 m s^{-1}. This consistently strong wind forcing could explain the start of ice breakup. Before ice motion is detected there are several decreases in air pressure aligned with shifting winds. These events do not appear to have enough force to overcome grounding strength of the ice. After motion in the ice is detected a period of warmer air temperatures is observed at yeardays 190–200. During this time the winds were predominantly westerly. Due to the length of time between ice motion and the onset of thaw, which we discuss in depth later, Harrison Bay in 2012 is also classified as thermal break up.

To take the comparison further, we calculated the correlation between each buoy velocity and the forcing parameters. Table 3-1 lists the correlation coefficients (r) between each buoy and the forcing parameters each year. The highest correlation was between 2012 Camden Bay buoy 3 with the water level (r = 0.46), but year-to-year the buoys are correlated with different variables. The correlation coefficients validate our comparison of the time series and were used to help classify the breakup as either mechanical or thermally driven. Typically, the buoy velocities were weakly correlated with the meridional wind component, except 2012 Buoy 2, 2015 Buoy 4 and all of the 2013 Camden Bay Buoys. In 2013 correlations were higher with meridional winds than zonal winds. This finding may indicate that a storm event, where winds are shifted from the predominantly easterly winds to either northerly or southerly winds can force the buoy and therefore ice movement from where it had remained fast.

Table 3-1 Correlation coefficients (*r*-values) between buoy velocity and forcing parameters. CB- Camden Bay, HB- Harrison Bay

Buoy Velocity	**Forcing Parameters**				
2007 CB	**Air Pressure**	**Air Temp**	**U Wind**	**V Wind**	**Water Level**
Buoy 1	-0.0982	0.0792	-0.0160	0.0030	0.0532
Buoy 2	-0.1540	0.1181	-0.0450	-0.0614	0.1580
Buoy 3	-0.1548	0.1595	-0.1297	0.0542	0.0306
Buoy 0	-0.1708	0.1619	0.1024	-0.0187	0.1683
2007 HB					
Buoy A	0.0106	0.1152	0.1384	-0.0042	0.0623
2008 CB					
Buoy 1	-0.1204	-0.0656	0.0434	0.1767	-0.0211
Buoy 2	-0.1524	-0.0538	0.0551	0.1616	-0.0546
Buoy 3	-0.1183	-0.0641	0.0201	0.0787	-0.0572
Buoy 4	-0.0205	0.0976	-0.1559	-0.0695	-0.0246
2009 CB					
Buoy 2	-0.0529	0.3050	0.0854	0.1637	0.1495
Buoy 3	0.0207	0.3291	0.0978	0.1649	0.1332
Buoy 4	0.0058	0.3803	0.1231	0.2233	0.2267
Buoy 4(2)	0.0023	0.3688	0.1453	0.1924	0.2269
2010 CB					
Buoy 1	-0.1785	-0.0960	-0.0819	-0.0397	0.0887
Buoy 2	-0.2506	0.1839	0.2189	0.0351	0.3328
Buoy 3	-0.2734	0.3067	0.2452	0.0716	0.4146
Buoy 3(2)	-0.2772	0.2802	0.1826	0.1134	0.4060
Buoy 4(2)	-0.2154	0.2797	0.1925	0.0358	0.4424
2010 HB					
Buoy A	-0.1005	0.0283	-0.0048	0.1354	0.0514
Buoy B	-0.2654	0.1884	0.2294	0.0171	0.3344
Buoy C	-0.1882	0.3892	0.3845	0.2137	0.3429
2012 CB					
Buoy 1	0.0927	0.0890	0.3334	0.1661	0.0278
Buoy 2	0.4174	0.0616	-0.4374	0.3275	-0.2681
Buoy 3	-0.1749	0.4260	0.4092	0.0018	0.4589
Buoy 4	-0.1326	0.2999	0.1241	0.0298	0.3408
2012 HB					
Buoy A	0.0722	0.0418	-0.1528	0.1064	-0.0615
Buoy B	-0.3037	0.3306	-0.0292	-0.0136	0.1396
Buoy C	-0.3210	0.2822	-0.0555	0.0542	0.1568
2013 CB					
Buoy 1	-0.3522	0.3650	0.1913	0.2300	0.2570
Buoy 2	-0.3359	0.4388	0.2187	0.2282	0.2604
Buoy 4	-0.2645	-0.0664	-0.2399	0.2650	0.1123
2013 HB					
Buoy A	0.0329	-0.0439	0.1395	0.1095	0.0506
Buoy B	0.2299	0.2853	0.1548	0.1007	0.3188
2014 CB					
Buoy 1	-0.0500	0.3455	0.1189	-0.0665	0.1296
Buoy 2	-0.0510	0.3767	0.1236	-0.0848	0.1255
2014 HB					
Buoy A	0.0534	0.1164	-0.1331	0.1597	0.0994
Buoy B	0.0413	0.0874	-0.1226	0.0357	0.0522
Buoy D	-0.1016	0.2253	-0.2161	-0.1257	-0.0956
2015 CB					
Buoy 00	-0.1465	0.1583	0.0959	-0.0253	0.2483
Buoy 0	-0.0418	0.0990	0.0108	0.1730	-0.1209
Buoy 4	-0.0565	0.0005	-0.3160	0.3095	-0.2371
2015 HB					
Buoy A	-0.0311	0.1707	-0.0563	0.2309	0.1252
Buoy B	0.0038	0.0089	-0.0884	0.0003	0.0016
Buoy D	-0.1107	0.0273	-0.1573	-0.0117	0.0488

Looking at the entire region to search for an overarching controlling mechanism through the period of our study, we employed a specific type of EOF analysis, PCA. We conducted a separate PCA on each of the two fast ice line study regions. Figures 3-8 show the results of the variance in each Eigen modes for each region. PCA revealed that the first Eigen mode explains 95.9% and 95.49% (Figure 3-7) of the variance in our two data matrices. This result means that, with the way the PCA method deconstructed each data matrix, the first Eigen mode returned can be used as a good approximation for the best way to represent our data. Again, air pressure, air temperature, and zonal wind velocity contain the most variability (Figure 3-9). Water level and buoy velocities explain almost no variance in the data matrices. From these results, we can conclude that over the nine-year period there is not one variable that dominates the variance with the buoy velocities. These results are expected given the differences in the correlation coefficients from year to year, where each buoy had different *r*–values (Table 3-1). The different pattern in variability between the buoy movement and forcing parameters, where the buoy

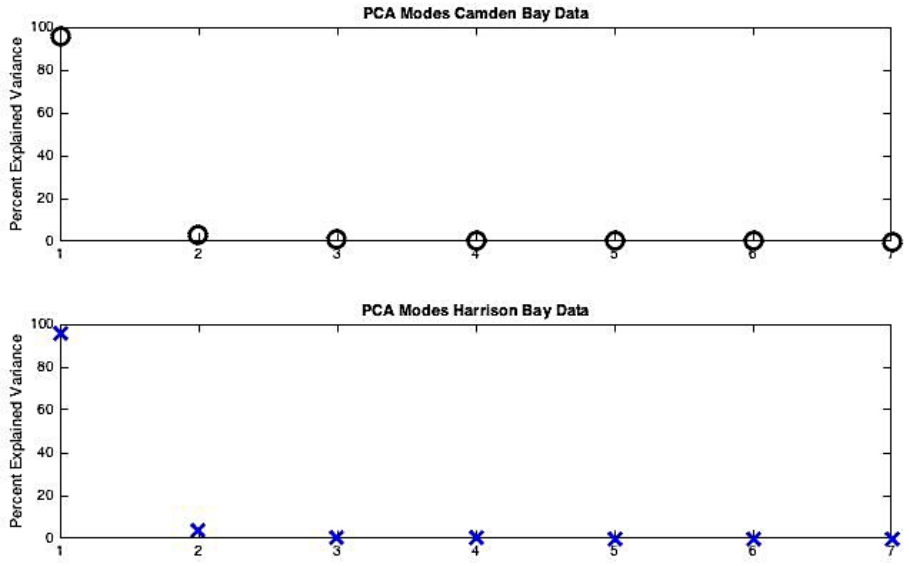

Figure 3-8 PCA modes plotted against the percent of explained variance in each mode, Camden Bay (upper) and Harrison Bay (lower).

velocity is approximately 0.0 m s^{-1} until breakup or a breakout event, and the forcing parameters, which show consistent variability over the breakup season, can explain the PCA results. A key difference between the methods concerns linearity. Correlation coefficients explain the linear relationship among the variables, while PCA explains the best relationship between modes orthogonal to each other, but the relationships or structures in the data does not have to be linear.

Finally, we compared the dates of thaw onset with start of breakup date for each bay and the entire region. The days since onset of thaw is a value that we can compare with previous studies to see how conditions in this region have changed over the last three decades. The onset of thaw is defined as the first day of a two-week period where the average air temperature allows for ice to begin thawing. Additionally, the start day must be above the thawing temperature. The freezing/thawing point of sea ice is controlled by salinity as well as temperature. On average a temperature of about –1.8°C is considered the salinity-determined freezing point in

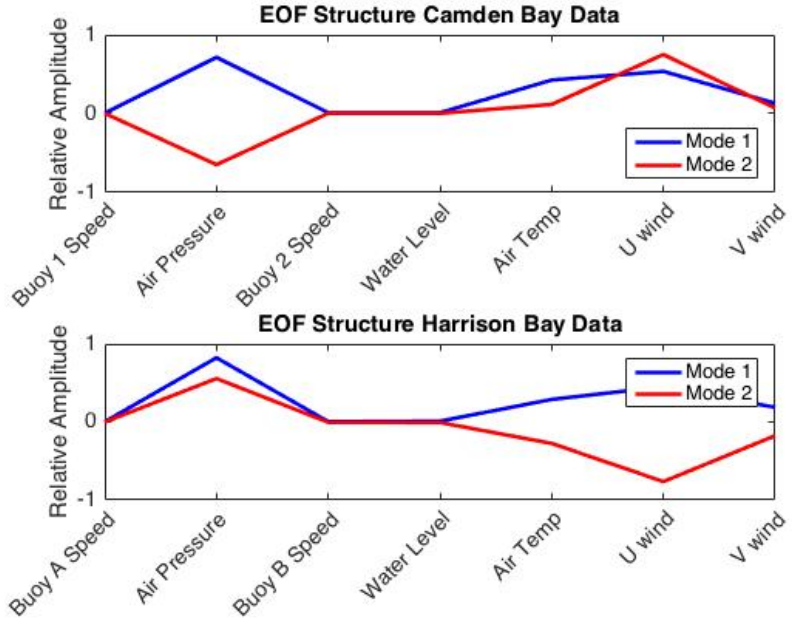

Figure 3-9 First two PCA modes of each region, Camden Bay (upper) and Harrison Bay (lower).

seawater (Wadham 2002), but for melting at the surface, a range of values from 0.0°C to –1.8°C has been used in previous studies to indicate the onset of thawing. Here, we followed Rigor and Hutching (2000) and set the thawing temperature threshold at –1.0 °C (Figure 2-6). The studies by Barry et al. (1979) and Mahoney et al. (2014) use 0.0°C reported from a nearby shore location. Our air temperature data were collected over the sea ice near the deployment location of each fast ice line.

3.4 Discussion of Breakup Mechanisms

In Camden Bay during 5 out of the 9 years in our study, landfast ice began moving before or on the date of thaw onset. In 2008, 2009, and 2012–2014 the buoys began moving before or within 15 days after the onset of thaw (Table 3-2). In Harrison Bay, however, the mean start of breakup occurred between 25 and 42 days after the onset of thawing temperatures. When we take the region as a whole, 5 of the 9 years had breakup starting less than 10 days after the onset of thaw or before the onset of that (Table 3-2). Averaged over the 9-year study period in Camden Bay the landfast ice began to break up 5 days after the onset of thaw. In contrast, in Harrison Bay the landfast ice did not start to breakup until 35 days after the onset of thaw. When averaged over the whole coastal region ice breakup occurred 10 days after the onset of thaw. Barry et al. (1979) reports that 55–140 thawing degree-days were needed to see openings and movement in the Beaufort Sea fast ice. Mahoney et al. (2014) reported that onset of thaw also occurred on average 10 to 15 days after the onset of thaw, which is in agreement with our results.

Table 3-2 Breakup start, onset of thaw, and number of days before or after the onset of thaw that breakup started

	Onset of Thaw DOY			Breakup Start DOY			Days Since Onset of Thaw		
Year	**Camden Bay**	**Harrison Bay**	**Regional Mean**	**Camden Bay**	**Harrison Bay**	**Regional Mean**	**Camden Bay**	**Harrison Bay**	**Regional Mean**
2007	152	153	152.5	188.5	186	180.4	36.5	33	27.9
2008	143	145	144	102.5	-	102.5	-40.5	-	-41.5
2009	146	144	145	137	-	137	-9	-	-8
2010	148	148	148	190.2	186.7	188.9	42.2	38.7	40.9
2011	141	143	142	168	-	168	27	-	26
2012	148	145	146.5	161.8	182.7	170.7	13.8	37.7	24.2
2013	148	147	147.5	111	188.5	154.4	-30	41.5	6.9
2014	128	136	132	122	162.3	146.2	-6	26.3	14.2
2015	133	134	133.5	149.3	176	162.7	16.3	42	29.2

Comparing these results with Mahoney et al. (2014) and their Figure 10, we show that our Camden Bay results align better with their results from the region to the east of Katovik where breakup started on or before the onset of thaw. The earlier breakup in Camden Bay could possibly be explained by the argument made by Mahoney and others that the eastern region of the Beaufort Sea coast has earlier breakup than the western region. Factors affecting the timing of breakup further to the east of Camden Bay, such as earlier thawing of the Mackenzie River in Canada and flooding coastal ice with fresh water, may be spreading west. Whereas in Harrison Bay there was thermal breakup of landfast ice occurring consistently over the 9-year study period. Another comparison of our results to those reported by Mahoney et al. (2014) shows that our trend in Harrison Bay is aligned with their observations from Nuiqsut, which is near our Harrison Bay fast ice line. Their results from the whole Beaufort Sea (zone 9) region reveal a trend to a later start of breakup near of Nuiqsut, and this later breakup takes place after the onset of thaw.

The differences between Camden Bay and Harrison Bay may be due to the distance of the 20-m isobath from shore. Overall Harrison Bay is shallow and has a higher amount of bottomfast ice (Barry et al. 1979), which can strengthen the landfast ice attachment. In Camden Bay, the 20-m isobath cuts close to towards the shore, and year to year about half of the buoys were deployed on ice in depths greater than 20 m, which could result in fewer grounded ridges at the SLIE. This result would have two effects on the landfast ice; with fewer grounded ridges holding the seaward edge of landfast ice fast to the sea floor it would not take as much force to break the landfast ice free (Mahoney et al., 2006), and incursions from the pack ice could impinge upon and break off the seaward edge with less chance of pressure ridges grounding in shallow water. Comparing the depth of water under sea ice where each buoy was deployed to the breakup date shows no clear trend in Camden Bay (Figure 17). In Harrison Bay there is a consistent timing of breakup without much change in depth under ice.

Throughout our 9-year study, we classified breakup as mechanical in 5 out of the 9 years in Camden Bay and thermal for all of the years in Harrison Bay. These conclusions were made from visual inspection of time series of buoy velocities, forcing variables and their correlations, and the number of days breakup occurred after the onset of thaw. Mahoney et al. (2007) over a study period of 1996–2004 reports no direct correlation between atmospheric events and breakup and concludes thermodynamic mechanisms were the main driver for timing of landfast ice breakup. It must be noted that in their study regional mean circulation and temperatures were compared with regional ice breakup. A direct comparison of results cannot be made because of the different techniques used and areas covered.

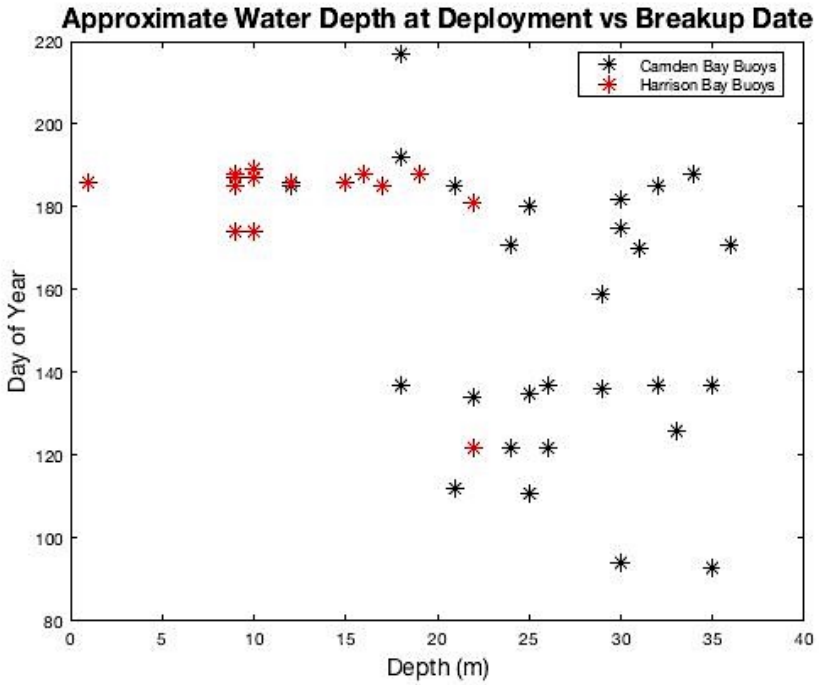

Figure 3-10 Average depth of water under ice where buoys were deployed compared with the day of year that buoy started to show ice breakup. Black stars are from Camden Bay fast ice line buoys. Red starts are from Harrison Bay fast ice lines. Depths were approximated from NOAA charts.

Chapter 4. SUMMARY

SVP buoys were deployed in landfast ice lines in two regions of the Alaska Beaufort Sea coast. With NAAR weather data and tidal gauge water level observations, we studied landfast ice breakup timing and dynamics over the period 2007–2015.

Hourly GPS positions from these buoys were used to calculate ice velocity; these velocities along with the positional track of the buoys were used to determine when the landfast ice began to breakup in each region. A regional average breakup date for the entire Alaska Beaufort Sea region and individual bay mean breakup dates were determined. Averaging the start date of breakup each year over the whole region, our results are in agreement with Mahoney (2014), with a very slight (2-day) shift to earlier breakup. We also found in the two regions examined a substantial difference in breakup timing. Harrison Bay had consistent breakup dates occurring around the first few days of July or last days of June each year. In Camden Bay, where there was more variability, breakup started as early as May in some years and as late as July in others. The variability between locations motivated us to study the differences between the two regions and processes affecting landfast ice breakup.

Visual examination of weather data from NARR and water level from a NOAA tide gauge compared with the timing of breakup in each bay showed that forcing events and breakup were in agreement with previous studies in Alaska (Petrich, 2012; Mahoney, 2014). To determine if there were any statistical connections between the forcing parameters and ice movement we calculated the linear correlation coefficients between buoy velocities and the

weather parameters. Then the PCA method was then used to test whether a correlation structure other than linear connects the ice movement variability with variability in the forcing parameters. Finally, we also calculated the onset of thaw date to determine how many days before or after the onset of thaw landfast ice broke free.

There were visual connections between weather events and ice movement in 2009, 2013, 2014 and 2015 in the Camden Bay region, but none in Harrison Bay. During these years in Camden Bay, the correlation coefficient was higher among one or multiple of the forcing parameters and buoy velocity (Table 3-1). For example, in 2013 all three buoy velocities had an $r = 0.25$ or greater with zonal winds and water levels. Moreover, in 2012 the Camden Bay buoys, except those nearest to shore, showed a higher correlation value with at least one forcing parameter.

The PCA results showed that the first mode accounts for 95% of the variability between the ice movement and chosen forcing variables. We could not determine an individual forcing parameter that accounted for the variability in the ice movement over the nine-year study period. The relative amplitude of the variability was mainly found in meridional winds and air pressure. Buoy velocity and water level for both the first and second mode explained almost none of the relative amplitude of the variability; i.e., the buoy velocity is approximately zero until the ice breaks free from the coast and remains approximately between 0.1 m s^{-1} and 1.0 m s^{-1}. Our other parameters showed more regular fluctuations in over shorter timescales; for example, the wind speed shows variability on scales of a day to about a week. This difference in timing of the variability among the forcing parameters, along with an inconsistent pattern in year to-year

breakup mechanisms accounts for the PCA results. This data analysis method confirmed the selected forcing parameters account for the ice breakup even though it demonstrated that there is no one overarching parameter affecting the breakup of landfast ice each year.

Determining the onset of thaw and adding this variable to the method comparing buoy velocity with forcing parameters, we classified breakup each year in each region as either mechanical or thermal. In Harrison Bay there was thermal breakup each year of the study. Ice remained fast to the shore until 20 + days after the onset of thaw. In Camden Bay 5 of the 9 years had mechanical breakup, where a storm or strong forcing event caused the ice to begin moving before or very soon after the onset of thaw.

Compared to previously published studies of landfast ice in this region during the past three decades, we report a similar trend in the start of breakup occurring earlier over the more recent 9- period of our study. We also report unique results indicating profound differences in breakup dates and dynamics in sub-regions of the Alaska Beaufort Sea coast. Continued monitoring of landfast ice conditions will allow a more robust analysis and confirm a trend toward earlier breakup of landfast ice.

BIBLIOGRAPHY

Barry, R. G., Moritz, R. E., & Rogers, J. C. (1979). The fast ice regimes of the Beaufort and Chukchi Sea coasts, Alaska. *Cold Regions Science and Technology, 1*(2), 129-152. doi:10.1016/0165-232x(79)90006-5

Druckenmiller, M. L., Eicken, H., Johnson, M. A., Pringle, D. J., & Williams, C. C. (2009). Toward an integrated coastal sea-ice observatory: System components and a case study at Barrow, Alaska. *Cold Regions Science and Technology, 56*(2-3), 61-72. doi:10.1016/j.coldregions.2008.12.003

Eicken, H., Salganek, M., Gradinger, R., Shirasawa, K., Perovich, D., & Leppäranta, M. (Eds.). (2010). *Field Techniques for Sea-Ice Research*. Fairbanks: University of Alaska Press.

Eicken, H., Kaufman, M., Krupnik, I., Pulsifer, P., Apangalook, L., Apangalook, P., . . . Leavitt, J. (2014). A framework and database for community sea ice observations in a changing Arctic: an Alaskan prototype for multiple users. *Polar Geography, 37*(1), 5-27. doi:10.1080/1088937x.2013.873090

Howell, S. E., Duguay, C. R., & Markus, T. (2009). Sea ice conditions and melt season duration variability within the Canadian Arctic Archipelago: 1979–2008. *Geophysical Research Letters, 36*(10). doi:10.1029/2009gl037681

Huang, L., Wolcott, D., & Yang, H. (2011). Tidal characteristics along the Western and Northern coasts of Alaska. In *US Hydro 2011 Conference, Florida*.

Jones, J., Eicken, H., Mahoney, A., Mv, R., Kambhamettu, C., Fukamachi, Y., . . . George, J. C. (2016). Landfast sea ice breakouts: Stabilizing ice features, oceanic and atmospheric forcing at Barrow, Alaska. *Continental Shelf Research, 126*, 50-63. doi:10.1016/j.csr.2016.07.015

Landsat 2 History. (n.d.). Retrieved May 3, 2017, from https://landsat.usgs.gov/landsat-2-history

Mahoney, A., Eicken, H., & Shapiro, L. (2007). How fast is landfast sea ice? A study of the attachment and detachment of nearshore ice at Barrow, Alaska. *Cold Regions Science and Technology, 47*(3), 233-255. doi:10.1016/j.coldregions.2006.09.005

Mahoney, A., Eicken, H., Shapiro, L., & Graves, A. (2006). Defining and locating the seaward landfast ice edge in northern Alaska. In *18th International Conference on Port and Ocean Engineering under Arctic Conditions (POAC'05), Potsdam, NY* (pp. 991-1001).

Mahoney, A. R., Eicken, H., Gaylord, A. G., & Gens, R. (2014). Landfast sea ice extent in the Chukchi and Beaufort Seas: The annual cycle and decadal variability. *Cold Regions Science and Technology, 103*, 41-56. doi:10.1016/j.coldregions.2014.03.003

Mahoney, A., Eicken, H., Gaylord, A. G., & Shapiro, L. (2007). Alaska landfast sea ice: Links with bathymetry and atmospheric circulation. *Journal of Geophysical Research, 112*(C2). doi:10.1029/2006jc003559

Matthews, J. B. (1981). Observations of surface and bottom currents in the Beaufort Sea near Prudhoe Bay, Alaska. *Journal of Geophysical Research, 86*(C7), 6653. doi:10.1029/jc086ic07p06653

Meier, W. N., Hovelsrud, G. K., Oort, B. E., Key, J. R., Kovacs, K. M., Michel, C., . . . Reist, J. D. (2014). Arctic sea ice in transformation: A review of recent observed changes and impacts on biology and human activity. *Reviews of Geophysics, 52*(3), 185-217. doi:10.1002/2013rg000431

MMS Home Page. (n.d.). Retrieved November 02, 2016, from http://boemre-new.gina.alaska.edu/

National Snow and Ice Data Center. (n.d.). Retrieved May 28, 2017, from http://nsidc.org/arcticseaicenews/charctic-interactive-sea-ice-graph/

National Snow and Ice Data Center. (1970, January 01). Retrieved November 02, 2016, from https://nsidc.org/data/docs/noaa/g02135_seaice_index/

Petrich, C., Eicken, H., Zhang, J., Krieger, J., Fukamachi, Y., & Ohshima, K. I. (2012). Coastal landfast sea ice decay and breakup in northern Alaska: Key processes and seasonal prediction. *Journal of Geophysical Research: Oceans, 117*(C2). doi:10.1029/2011jc007339

Petty, A. A., Hutchings, J. K., Richter-Menge, J. A., & Tschudi, M. A. (2016). Sea ice circulation around the Beaufort Gyre: The changing role of wind forcing and the sea ice state. *Journal of Geophysical Research: Oceans, 121*(5), 3278-3296. doi:10.1002/2015jc010903

Reimnitz, E. (2002): Interaction of River Discharge with Sea Ice in Proximity of Arctic Deltas: A Review , Polarforschung, Bremerhaven, Alfred Wegener Institute for Polar and Marine Research & German Society of Polar Research, 70 , pp. 123-134 .

Reimnitz, E., Toimil, L., & Barnes, P. (1978). Arctic continental shelf morphology related to sea-ice zonation, Beaufort Sea, Alaska. *Marine Geology, 28*(3-4), 179-210. doi:10.1016/0025-3227(78)90018-x

Reimnitz, E., Dethleff, D., & Nürnberg, D. (1994). Contrasts in Arctic shelf sea-ice regimes and some implications: Beaufort Sea versus Laptev Sea. *Marine Geology, 119*(3-4), 215-225. doi:10.1016/0025-3227(94)90182-1

Rigor, I. G., Colony, R. L., & Martin, S. (2000). Variations in Surface Air Temperature

Observations in the Arctic, 1979–97. *Journal of Climate, 13*(5), 896-914. doi:10.1175/1520-0442(2000)013<0896:visato>2.0.co;2

Seasonal to decadal predictions of arctic sea ice: challenges and strategies. (2012). Washington, D.C.: National Academies Press.

Selyuzhenok, V., Krumpen, T., Mahoney, A., Janout, M., & Gerdes, R. (2015). Seasonal and interannual variability of fast ice extent in the southeastern Laptev Sea between 1999 and 2013. *Journal of Geophysical Research: Oceans, 120*(12), 7791-7806. doi:10.1002/2015jc011135

Squire, V. A. (1993). The breakup of shore fast sea ice. *Cold Regions Science and Technology, 21*(3), 211-218. doi:10.1016/0165-232x(93)90065-g

Stroeve, J. C., Markus, T., Boisvert, L., Miller, J., & Barrett, A. (2014). Changes in Arctic melt season and implications for sea ice loss. *Geophysical Research Letters, 41*(4), 1216-1225. doi:10.1002/2013gl058951

The Multispectral Scanner System. (n.d.). Retrieved May 3, 2017, from https://landsat.gsfc.nasa.gov/the-multispectral-scanner-system/

Thomson, R. E., & Emery, W. J. (2014). *Data analysis methods in physical oceanography*. Amsterdam: Elsevier.

Vaudrey, K. (1985). 1985-86 Ice Motion measurements in Camden Bay, AOGA Project 328Aa, Vaudrey & Associates. *Inc. San Luis Obispo, CA*.

Vaudrey, K. (2006). Multiyear Ice Statistics for the Beaufort and Chukchi Seas, Vaudrey & Associates. *Inc. San Luis Obispo, CA*.

Wadhams, P. (2002). *Ice in the ocean*. Australia: Gordon and Breach Science.

Weingartner, T. J., Okkonen, S. R., & Danielson, S. L. (2005). *Circulation and water property variations in the nearshore Alaskan Beaufort Sea*. US Department of Interior, Minerals Management Service, Alaska Outer Continental Shelf Region.

Williams, W. J., & Carmack, E. C. (2015). The 'interior' shelves of the Arctic Ocean: Physical oceanographic setting, climatology and effects of sea-ice retreat on cross-shelf exchange. *Progress in Oceanography, 139*, 24-41. doi:10.1016/j.pocean.2015.07.008